Isotope (Sr, C) and U-Pb SHRIMP zircon geochronology of marble-bearing sedimentary series in the Eastern Sierras Pampeanas, Argentina. Constraining the SW Gondwana margin in Ediacaran to early Cambrian times.

Juan A. Murra[a], Cesar Casquet[b,c], Francisco Locati[a], Carmen Galindo[b,c], Edgardo G. Baldo[a], Robert J. Pankhurst[d], Carlos W. Rapela[e]

[a] Centro de Investigaciones en Ciencias de la Tierra (CICTERRA), CONICET, Universidad Nacional de Córdoba, Córdoba, Argentina.

[b] Departamento de Petrología y Geoquímica. Universidad Complutense, 28040 Madrid, Spain

[c] Instituto de Geociencias (IGEO), CSIC, UCM. 28040 Madrid, Spain.

[d] Visiting Research Associate, British Geological Survey, Keyworth, Nottingham NG12 5GG, UK.

[e] Centro de Investigaciones Geológicas, CONICET, Universidad Nacional de la Plata, 1900 La Plata, Argentina.

ABSTRACT

The Sierras de Córdoba Metasedimentary Series consists of marbles and metasiliciclastic rocks of Ediacaran to early Cambrian age (ca. 630 and 540 Ma) that underwent high-grade metamorphism during the collisional Pampean orogeny in the early Cambrian. The ages of the marbles were determined from the Sr-isotope composition (blind dating) of screened samples of almost pure calcite marble and were further constrained with C- and O-isotope data and U-Pb SHRIMP detrital zircon ages of an interbedded paragneiss. Two groups of samples are recognized with Sr-isotope composition ca. 0.7075 and 0.7085 that are considered stratigraphically significant. The first is inferred early Ediacaran, the second late Ediacaran to early Cambrian. The Sierras de

Córdoba Metasedimentary Series is correlated for the first time with marble-bearing metasedimentary series in several sierras to the west and north of Sierras de Córdoba (e.g., the Difunta Correa Sedimentary Sequence and the Ancaján Series), implying that all were probably parts of an originally extensive sedimentary cover. These series bear evidence of sedimentary sources in the Mesoproterozoic (and Paleoproterozoic) basement of the Western Sierras Pampeanas (part of the large MARA continental block) and farther west (Laurentia?). In terms of the age of limestones/marbles and detrital zircon patterns, the Sierras de Córdoba Metasedimentary Series differs strongly from the older section of late Ediacaran to early Cambrian Puncoviscana Formation of northwestern Argentina, which outcrops in northern Sierra Chica and Sierra Norte, with sedimentary input from western Gondwana sources.

The Sierras de Córdoba Metasedimentary Series and the Puncoviscana Formation were probably juxtaposed during the Pampean orogeny along a complex suture zone that was further folded and/or imbricated at mid-crustal depths. The peak of metamorphism was attained at 527 ± 2 Ma. According to the evidence found here most of the Sierras Pampeanas to the west of the Sierras de Córdoba were part of the lower colliding plate during the final amalgamation of SW Gondwana.

Keywords: Ediacaran carbonates, Sr-isotope blind dating, U-Pb SHRIMP zircon geochronology, Sierras Pampeanas, SW Gondwana

1. Introduction

The Sierras Pampeanas of western and northwestern Argentina extend over a large N-S elongated area some 700 km long and 450 km wide (Fig. 1). The basement in this area consists of Palaeozoic to Mesoproterozoic igneous and metamorphic rocks. Minor outcrops of basement are also found in other structural units of the Andean foreland, e.g., the Precordillera and the Puna.

Unfossiliferous metasedimentary rocks are abundant in the basement, most of them displaying low- to high-grade regional metamorphism of different ages (see Rapela et al., 1998a; 2001; Ramos et al., 2010 for a review). Siliciclastic rocks are widespread, but marbles and calc-silicate rocks can be locally abundant. The latter represent former deposits of marine carbonates and provide constraints for stratigraphy and paleogeography through the application of isotope geochemistry methods (Sr, C and O) (Galindo et al., 2004; López de Azarevich 2010; Murra et al., 2011 and references therein).

The Sr-isotope composition of marbles that remain unmodified after sedimentation has been increasingly used for chemical stratigraphy since the seminal work of Burke et al. (1982). These authors showed that this ratio in open-ocean limestone increased non-linearly over time because of a general predominance of input from continental radiogenic Sr compared to a juvenile contribution from the oceanic crust. Determination of $^{87}Sr/^{86}Sr$ has been particularly useful for dating Neoproterozoic and older carbonates where fossils are absent. Several compilations have been published showing the Sr-isotope composition of seawater *vs*. time for the Neoproterozoic era, some of them accompanied by $\delta^{13}C$ values (and S and O-isotope systematics), to constrain the age of paleoclimatic changes (e.g., Derry et al., 1989, 1992; Jacobsen and Kauffman, 1999; Kuznetsov, 1998; Kuznetsov et al., 2013; Montañez et al., 2000; Halverson et al., 2007, 2010, among others).

We focus here on the Sr, C and O-isotope composition of marbles from the Sierras de Córdoba and easternmost Sierra de San Luis (Eastern Sierras Pampeanas, ESP) (Figs. 1 and 2) and secondly on U-Pb SHRIMP zircon dating of interbedded metasiliciclastic rocks. It is the first time that this type of research has been carried out over such an extended region of the Sierras Pampeanas. Our results are significant for the provenance and timing of deposition, correlation with

71 carbonate sequences elsewhere in the Sierras Pampeanas, and the tectonic evolution of the
72 continental margin of SW Gondwana leading up to the Pampean orogeny.
73
74 **2. Geological setting**
75 The Sierras Pampeanas of Argentina can be divided into two groups separated by the
76 Bermejo-Desaguadero first-order fault (Fig. 1):
77 1) the Western Sierras Pampeanas (WSP) consist of a Mesoproterozoic (and probably
78 reworked Paleoproterozoic) basement of metabasites, orthogneisses, metasedimentary rocks
79 (mainly gneisses and psammites with a few marbles), and massif-type anorthosites (Pankhurst and
80 Rapela, 1998; Vujovich et al., 2004; Casquet et al., 2004, 2008; Rapela et al., 2010) with a
81 Neoproterozoic metasedimentary cover called the Difunta Correa Sedimentary Sequence including
82 abundant marbles (Varela et al., 2001; Galindo et al., 2004). Both basement and cover experienced
83 deformation and low- to high-grade metamorphism in the Famatinian orogeny (Early to middle
84 Ordovician);
85 2) the Eastern Sierras Pampeanas consist of low to high-grade metasedimentary and plutonic
86 rocks. The eastern part of the Eastern Sierras Pampeanas underwent Pampean orogeny (low- to
87 high-grade metamorphism and magmatism) between 545 and 520 Ma (latest Ediacaran to early
88 Cambrian), and was variably reworked by the Famatinian orogeny. The western part of the Eastern
89 Sierras Pampeanas underwent the Famatinian orogeny only with abundant magmatism and low- to
90 high-grade metamorphism from ~490 to 430 Ma (Sims et al., 1998; Pankhurst et al., 1998; Rapela
91 et al., 1998a, 2007; Dahlquist et al., 2008).
92 The oldest sedimentary protoliths in the easternmost part of the Eastern Sierras Pampeanas
93 (phyllites to gneisses and metapsammites) have been correlated with the Puncoviscana Formation of
94 northwestern Argentina (Cordillera Oriental). The Puncoviscana Formation basically is a sequence

of pelitic-greywacke turbidites with locally interbedded conglomerates, limestones and volcanic rocks of late Neoproterozoic to Cambrian age (Omarini et al., 1999; Do Campo and Ribeiro Guevara, 2005; Toselli et al., 2005, 2010; Zimmermann, 2005; Adams et al., 2008; Escayola et al., 2011, among others). In the western Eastern Sierras Pampeanas two metasedimentary series are found. A late Neoproterozoic sequence with marbles (the Ancaján Series) in the sierras of Ancaján and Ancasti (Fig. 1) is isotopically equivalent to the Difunta Correa Sedimentary Sequence of the Western Sierras Pampeanas (Murra et al., 2011; Rapela et al., 2016), whereas a sequence of typically banded schists (the Ancasti Series) is equivalent to the Puncoviscana Formation. Both have been informally termed as the Puncoviscan series (Rapela et al., 2007, 2016) and both underwent low- to high-grade Famatinian metamorphism and deformation only, with no evidence so far of significant Pampean metamorphism. The contact between the two series is highly strained, suggesting tectonic juxtaposition.

3. Sierras de Córdoba Metasedimentary Series

The Sierras de Córdoba are the easternmost outcrops of the Eastern Sierras Pampeanas (Fig. 1). They consist of metasedimentary rocks, orthogneisses and plutonic rocks and dykes, locally covered by continental sediments of Carboniferous-Permian, Cretaceous and Cenozoic ages. The metasedimentary rocks are metapelites and metapsammites interbedded with widespread marbles and calc-silicate rocks (Gordillo, 1984; Gordillo and Bonalumi, 1987; Baldo, 1992; Guereschi and Martino, 2002, 2003). Plutonism, deformation and metamorphism took place in the early Cambrian Pampean orogeny (Rapela et al., 1998b). Metamorphism reached medium to high temperature (600-800 °C) and intermediate pressure (4-8 kbar) (Gordillo and Lencinas 1979; Rapela et al., 1998b, 2002; Steenken et al., 2010). Marbles are found as lenticular bodies due to stretching, but they can be followed over long distances with thicknesses from a few centimetres to hundreds of metres.

119 They are often spatially associated with ductile shear zones and mafic to ultramafic igneous rocks
120 (Martino, 2003). We will refer to this marble-bearing sequence as the "Sierras de Córdoba
121 Metasedimentary Series". Metasedimentary rocks equivalent to the Puncoviscana Formation of NW
122 Argentina were recognized in the Sierras de Córdoba (Sierra Grande and in northwestern Sierra
123 Chica and Sierra Norte) (Fig. 2) on the basis of detrital zircon ages (Escayola et al., 2007; Rapela et
124 al., 2007, 2016). The term Puncoviscana Formation in the literature embraces sedimentary rocks
125 probably older, coeval and younger than the Pampean magmatic arc, with the only constraint that
126 they are older than the unconformably overlying middle to late Cambrian Meson Group (e.g.,
127 Omarini et al., 1999; Adams et al., 2008, 2011; Escayola et al., 2011, and references therein). We
128 restrict the term here to that part of the siliciclastic succession that is of relevance to the early
129 history of the Puncoviscana sedimentary basin (e.g., Casquet et al., 2012). These rocks host the
130 magmatic arc in the south (540-530 Ma) and can be coeval with syn-orogenic volcanism (ca. 530
131 Ma) in the north (Escayola et al., 2011).
132 The detrital zircon age pattern in the Eastern Sierras Pampeanas is almost bimodal with
133 characteristic peaks at ca. 1000 and 600 Ma. The zircon was interpreted as derived from West
134 Gondwana sources in the east (Natal-Namaqua belt and probably the Brasiliano-Panafrican orogen
135 and the huge East African orogen) (Rapela et al., 2016). The maximum sedimentation age is 570
136 Ma and the uppermost part of the series contains interbedded tuffs of ca. 537 Ma (Escayola et al.,
137 2011; von Gossen et al., 2014). Early Pampean orogeny magmatism in the Sierra Chica and Sierra
138 Norte of Córdoba took place between 540 and 530 Ma (Rapela et al., 1998b; Schwartz et al., 2008;
139 Iannizzotto et al., 2011). The relationship (age and structure) between the Puncoviscana Formation
140 and the marble-bearing Sierras de Córdoba Metasedimentary Series has so far not been defined.
141 The $^{87}Sr/^{86}Sr$ values and the C (and O-isotope in lesser degree) composition of limestones
142 from the Puncoviscana Formation in NW Argentina suggest that they are early Cambrian (Sial et

143 al., 2001; Lopez de Azarevich et al., 2010; Toselli et al., 2012), consistent with the age of
144 sedimentation between ca. 570 and 537 Ma yielded by the ages of detrital zircons in interbedded
145 schists (Escayola et al., 2011; Casquet et al., 2012; Rapela et al., 2016). However, marbles of the
146 Ancaján Series in the western Eastern Sierras Pampeanas (Sierra de Ancasti) yielded Sr-isotope
147 ratios corresponding to the Ediacaran (Toselli et al., 2010; Murra et al., 2011), and the same Sr-
148 isotope composition was found in marbles from the Difunta Correa Sedimentary Sequence in the
149 Western Sierras Pampeanas (Sierras de Pie de Palo, Maz and Umango; Fig. 1) (Varela et al., 2001;
150 Galindo et al., 2004). Recently Rapela et al. (2016) have confirmed that similarities between these
151 two older series extend to the detrital zircon age patterns of siliciclastic rocks interbedded with the
152 marbles and that these patterns differ from that of the Puncoviscana Formation. The Difunta Correa
153 Sedimentary Sequence is thus apparently equivalent to the Ancaján Series, representing deposition
154 across the tectonic boundary between the two groups of the Sierras Pampeanas (Fig. 1).
155

156 **4. Sampling and analytical techniques**

157 Sampling was designed to include most of the marble outcrops of the Sierras de Córdoba and
158 easternmost Sierra de San Luis (Fig. 2). A total of 141 samples were collected, of which 49 were
159 selected for petrography and chemistry. One sample was collected of migmatite interbedded with
160 marble (Fig. 2) for U-Pb SHRIMP zircon geochronology to better constrain the age of the Sierras de
161 Córdoba Metasedimentary Series and to strengthen correlations with sedimentary successions
162 elsewhere in the Sierras Pampeanas.

163 To initially estimate the amount of calcite and dolomite, slabs (6 x 4 cm) were cut and the
164 surface stained with alizarin (0.3 g of alizarin in 100 ml of 1.5% HCl solution) for 4 minutes and
165 then gently washed in distilled water. The percentage of stained calcite in the slab surface was
166 determined by computer imaging (using Image-J 1.48v, Rasband 1997-2015). Samples with calcite

167 > 70% (n = 33) were selected (Table 1). They were then analysed as in Murra et al. (2011) for Ca,
168 Mg, Mn and Fe, and the insoluble residuum (IR) determined. Samples with low IR values were
169 chemically screened according to the Mn/Sr, Mg/Ca and Fe/Sr ratios (Brand and Veizer, 1980;
170 Melezhik et al., 2001 and references therein) to further select those that had not undergone
171 significant post-sedimentary changes (Table 2): these were analysed for Sr, C and O-isotope
172 composition.

173 Sr-isotope composition was determined at the Geochronology and Isotope Geochemistry
174 Centre of the Complutense University, Madrid. To exclude contamination from other minerals,
175 carbonate samples (~ 30 mg) were leached in a 10% acetic acid solution and then centrifuged to
176 remove the insoluble residue (Fuenlabrada and Galindo, 2001). Additionally, the insoluble residue
177 (IR as wt%) was determined. The solution was subsequently evaporated and then dissolved in 3 ml
178 of 2.5 N HCl. Sr was separated using cation-exchange columns filled with BioRad® 50W X12
179 (200/400 mesh) resin. Procedural blank was less than 2 ng for Sr. The Sr-isotope composition was
180 determined on an automated multicollector SECTOR 54® mass spectrometer and $^{87}Sr/^{86}Sr$ values
181 were normalized to a $^{86}Sr/^{88}Sr$ value of 0.1194. The NBS-987 standard was routinely analysed along
182 with our samples and gave an average $^{87}Sr/^{86}Sr$ value of 0.710251 ± 0.00002 (2σ, n=7). Individual
183 precision estimates (standard error on the mean) are given in Table 2; overall analytical uncertainty
184 is estimated to be ± 0.01%. Most of the O and C-isotope determinations (n = 15) were carried out
185 on a double inlet Micromass SIRA-II® mass spectrometer at the Isotope Laboratory of Salamanca
186 University (ILSU) following the method of McCrea (1950). Three samples (Q-09, IG-102 and IGU-
187 178) were analysed using direct injection into a GasBench/MAT-23 Mass spectrometer at the CAB
188 (Centro de Astrobiología, CSIC). Rocks were first reacted with 100% orthophosphoric acid at 25ºC
189 to liberate CO_2. O-isotope compositions were corrected following Craig (1957). O and C-isotope
190 compositions are reported in δ (‰) notation on the PDB scale. Analytical errors (1σ) are ± 0.057‰

191 for C and ± 0.198‰ for O (ILSU) and 0.035‰ for C and 0.1‰ for O (CAB). Results are shown in
192 Table 2.

193 Rb was determined in four samples with different Sr contents and Sr-isotope compositions to
194 check for the effect of ^{87}Rb decay on the initial Sr-isotope composition. The samples were reacted
195 with 0.5 M acetic acid, centrifuged at 4000 rpm and the leachate collected for analysis. The residue
196 was washed twice with millipore water centrifuged and the new leachate added to the first. The
197 leachates were dried and re-dissolved with 1 ml of 0.1 M HNO_3 for analysis by ICP-MS. All four
198 samples yielded Rb contents below detection limit, i.e., <0.2 ppm.

199 Sample LC-158 was analysed at the Centro de Instrumentación Científica of Granada (Spain)
200 using SHRIMP IIe/mc, following the method described by Montero et al. (2014). Results are shown
201 in figure 9 as Tera-Wasserburg and density probability plots produced using ISOPLOT/Ex
202 (Ludwig, 2003). For ages less than 1.1 Ga the ^{207}Pb-corrected $^{206}Pb/^{238}U$ age (Williams, 1998) was
203 preferred; otherwise choice between the ^{204}Pb-corrected $^{206}Pb/^{238}U$ and $^{207}Pb/^{206}Pb$ age was based
204 on the relative age uncertainty, discounting any that were >10% discordant (Table 3).

205

206 **5. Marble outcrops and petrography**

207 The main marble outcrops are concentrated in the central-eastern Sierras de Córdoba defining
208 two main belts: the Sierra Chica belt on the east and the Sierra Grande belt on the west. The two
209 belts are separated by the Valle de Punilla – Calamuchita Cenozoic thrust system. The Sierra Chica
210 belt shows the more abundant marble outcrops. The Sierra Grande belt runs to the north and west of
211 the large Devonian Achala batholith (Fig. 2) (Lira and Sfragulla 2014 and references therein). Small
212 marble outcrops are also found in the southern part of Sierra Grande and the easternmost Sierra de
213 San Luis (Costa et al., 2001) (Fig. 2). The outcrops are tectonically repeated by folding and/or

214 thrusting, and often isolated because of stretching (boudinage): their original disposition remains
215 unknown.

216 Most samples were collected in quarries, either inactive or still exploited for various uses such
217 as the cement industry (e.g., Fig. 3). In all cases the host rocks are migmatites, gneisses, schists and
218 calc-silicate rocks (Bonalumi et al., 1999). Marbles are white to pink and medium to coarse-grained.
219 A decimetre-scale banding between almost pure and impure marble is common (Table 1, Figs. 3
220 and 4). Mineral composition can be summarized as: Cal (73-98% modal) ± Dol – Qz – Di – Tr –
221 Phl – Ttn – Gr – Tlc – Wo – Opq (mineral abbreviations after Whitney and Evans 2010). Texture is
222 granoblastic with calcite grains 0.5 mm in size on average, evolving into porphyroclastic with grain-
223 size reduction near the shear zones. In some outcrops in central Sierra Chica ca. 1 m thick dykes of
224 fine-grained tonalite of unknown age intruded the marbles. Other rocks found within the marble
225 outcrops are disrupted amphibolite lenses 5 to 20 m long and sporadic layers of impure
226 metapsammite and/or quartzite.

227 The migmatite sample (LC-158) for U-Pb SHRIMP zircon geochronology was collected from
228 a succession of gneisses and migmatites interbedded with amphibolites and marbles at La Calera
229 near Córdoba (Baldo et al., 1996) (Table 1, Fig. 2 and 5). It is a metatexite consisting of Qz – Grt –
230 Pl – Bt – ± Sil, with Zrn – Ep – Opq – Ap accessories. Foliation is defined by granoblastic Qz + Pl
231 lenses alternating with biotite–rich bands that wrap around garnet porphyroclasts up to 2 mm in
232 size. The latter contain inclusions of biotite, quartz and sillimanite.

233

234 **6. Isotope composition**

235 *The Sierra Chica belt.* Seventeen samples were analysed from this belt. They are calcite
236 marbles with contents of Ca = 30.45 – 51.41 wt%; Mg = 0.002 – 0.768 wt%; Sr = 324 – 1828 ppm,
237 Fe = 297 – 2351 ppm and Mn between <1 and 255 ppm (Table 2). The content of non-carbonate

minerals (as insoluble residue, IR) is low, between 0.14 and 4.47 wt% (Table 2). The higher IR values (e.g., in samples Q-27 and SMi-87) correlate with decreased Ca and increased Mg and Mn; Fe contents are also relatively high. This evidence suggests that at least part of the Mg, Mn and Fe is contributed by the non-carbonate fraction of the marble. Most samples show Mn/Sr, Mg/Ca and Fe/Sr ratios compatible with little post-sedimentary alteration (Table 2 and Fig. 6). Only three samples show one or two elemental ratios higher than the boundary values for absence of alteration (Q-21, SA-26, SMi-87). The $^{87}Sr/^{86}Sr$ ratios of the seventeen samples fall into two groups: ten samples between 0.70834 and 0.70860 and seven samples between 0.70747 and 0.70771, well outside error limits and the difference is therefore considered geologically significant (Table 2, Fig. 6). Measured Rb contents of four samples of the first group are negligible (<0.2 ppm) and cannot have contributed to the higher $^{87}Sr/^{86}Sr$ ratios. Moreover, one of the three samples with relatively high elemental ratios referred to above is in the low $^{87}Sr/^{86}Sr$ group, suggesting that small amounts of alteration have had minimal effect on Sr-isotope composition. C and O-isotopes were determined in twelve samples. The $\delta^{13} C_{PDB}$ value ranges from -0.16 to +3.54‰, compatible with a marine origin. All the samples with the more radiogenic Sr show positive values of $\delta^{13} C_{PDB}$, whereas the less radiogenic group shows both positive and negative values. The $\delta^{18}O_{PDB}$ values range from -6.03 to -12.05‰ (most values > -10‰), again suggesting little modification of the original marine composition (Table 2). The $\delta^{18}O$ values of late Neoproterozoic carbonates are < -5‰ (e.g., Jacobsen and Kauffmann, 1999). Values larger than -10‰ are considered indicative of little post-sedimentary alteration (Letnikova et al., 2011). The lowest value (-12.05‰), from the anomalous sample SMi-87, may reflect some devolatilization during regional metamorphism.

The Sierra Grande belt. The samples from this area are often dolomitic and only seven, from three specific sectors, were considered suitable for analysis (Fig. 2). These are calcite marbles with contents of Ca = 31.92 – 40.72 wt%, Mg = 0.01 – 0.507 wt%, Sr = 828 – 3513 ppm; Fe = 11 – 59

ppm and Mn = 0.35 – 8.71 ppm (most < 1 ppm Mn) (Table 2). In all cases the Mn/Sr, Mg/Ca and Fe/Sr ratios and the IR values are low or very low, suggesting that the rocks did not undergo significant post-sedimentary alteration (Table 2, Fig.6). Five samples yielded $^{87}Sr/^{86}Sr$ ratios values between 0.70737 and 0.70740, similar to but slightly lower than those of the Sierra Chica belt, and two yielded 0.70836 and 0.70848 (Table 2, Fig. 6). C and O-isotope compositions of three samples ($\delta^{13}C_{PDB}$ = +0.73 to +3.2‰; $\delta^{18}O_{PDB}$ = -4.86 to -9.14‰, Table 2) again suggest little post-sedimentary alteration of former marine limestones.

Other outcrops. Marbles from Cienaga del Coro were not considered because they are dolomitic. Four samples were analysed from the other sectors: two from Achiras and two from San Luis. They are calcite marbles with contents of Ca = 37.95 – 35.52 wt%; Mg = 0.08 – 0.77 wt%; Sr = 305 – 2106 ppm; Fe = 305 – 343 ppm and Mn = 0.2 – 126 ppm (Table 2). None of the samples yielded Mn/Sr, Mg/Ca and Fe/Sr ratios indicative of significant post-sedimentary changes. IR values range from 1.25 to 6.03 wt%, i.e., slightly higher than in the other two belts (Table 2 and Fig. 6). Three samples have $^{87}Sr/^{86}Sr$ ratios of 0.70743 to 0.70764 and one gave 0.70786, mostly within the range of the less radiogenic group recognized in the other two belts. C and O-isotope composition of one sample ($\delta^{13}C_{PDB}$ ~ +2.78‰; $\delta^{18}O_{PDB}$ ~ -7.91‰, Table 2) are also similar to those described before.

7. U-Pb SHRIMP zircon geochronology

Fifty six spots were analysed in sample LC-158 (Table 3). Two textural types of zircon were recognized (Fig. 7). The first consists of elongated grains (80 to 150 μm) often with a core showing oscillatory zoning and a discordant overgrowth with variable cathodo-luminiscence (CL). The second group consists of equant grains (20 to 100 μm), sometimes internally simple with low CL and complex sector-zoning, or composite with a homogenous low-CL core and a low-CL zoned

286 rim. The first group has high Th/U ratios (0.14 – 1.89) typical of igneous zircons and ages between
287 ca. 700 and 1650 Ma; there is a notable peak at ca.1190 Ma (range 1100–1250 Ma), and an older
288 population with ages of ca. 1950–2060 Ma (Fig. 8). The second group shows typical high-grade
289 metamorphic zoning (e.g., Harley et al., 2007), low Th/U ratios between 0.02 and 0.05 and ages
290 between 514 and 535 Ma, i.e., early to middle Cambrian (Terreneuvian and Series 2, according to
291 the 2015 IUGS chronostratigraphic chart). One spot with an unrealistic low age (ca. 300 Ma) was
292 not considered. A weighted mean age for the second group is 527 ± 2 Ma (n=14; MSWD = 2.2)
293 (Fig. 8a). Rims were not analysed because of their small thickness.
294
295 **8. Discussion**
296 Recent compilations of Sr and C (and O-isotope in lesser degree) composition in Phanerozoic
297 and Proterozoic seawater show trends that can be used to estimate the age of unfossiliferous marine
298 carbonates assuming that they preserved original compositions unmodified by diagenesis and
299 metamorphism (Veizer et al., 1999; Jacobsen y Kaufman, 1999; Montañez et al., 2000; Melezhik et
300 al., 2001; Jiang et al., 2007; Prokoph et al., 2008; Halverson et al., 2010). The method is particularly
301 useful for periods where the fossil evidence is scarce or absent, as is usually the case for Proterozoic
302 rocks. The $^{87}Sr/^{86}Sr$ ratio and the C-isotope composition are widely used, the first for dating (blind
303 dating) and the second to infer paleoenvironmental conditions. The O-isotope composition however
304 can be more easily modified through interaction with meteoric water and high-temperature
305 percolating fluids (Fairchild et al., 1990). Despite the relative vulnerability of carbonates to
306 diagenetic and metamorphic processes, they can often retain the original isotope compositions even
307 under medium- to high-grade conditions (Brand and Veizer, 1980; Melezhik et al., 2001).
308
309 *8.1- Geochemical evidence*

310 The Mg content is very low in all the samples (<1 wt%), indicating that calcite is the only
311 carbonate present or is the most abundant (Mg/Ca is in fact lower than 0.03 in all samples).
312 Moreover, the content of impurities as estimated from the insoluble residue is generally less than 3
313 wt%, in many cases <1 wt%) (Table 2). The main accessory minerals are quartz, phlogopite, opaque
314 minerals, tremolite and diopside, along with others found at trace levels (Table 1). The moderate to
315 high contents of Sr (300-3500 ppm), the very low Rb values (<0.2 ppm), the $^{87}Sr/^{86}Sr$ values, the
316 Mg/Ca, Mn/Sr and Fe/Sr ratios, the low Mn contents and the C and O-isotope compositions all
317 suggest that the rocks underwent minor post-sedimentary alteration and that protoliths were marine
318 calcite and aragonite limestones. Therefore dating based on comparison of the $^{87}Sr/^{86}Sr$ values with
319 existing compilations should yield acceptable constraints on the ages of sedimentation. C-isotopes
320 can help to better constrain the chronology.
321 The $^{87}Sr/^{86}Sr$ values of the Sierra de Córdoba marbles fall between 0.70736 and 0.70786 (16
322 samples) and between 0.70834 and 0.70860 (12 samples). There is no clear geographical separation
323 of the two groups; while the more radiogenic group appears to be predominant in the east and the
324 less radiogenic in the west (Fig. 2) further sampling is needed to confirm this issue. Figure 9a shows
325 the compilation of $^{87}Sr/^{86}Sr$ and C-isotope values of seawater for the late Proterozoic to the
326 Cambrian/Ordovician boundary according to Halverson et al. (2010) and Kuznetsov et al. (2013).
327 The less radiogenic group of $^{87}Sr/^{86}Sr$ values is uniquely coincident with seawater composition at
328 620-635 Ma, i.e., early Ediacaran. We note that it has recently been demonstrated that carbonates in
329 the Bambui Group of the southern San Francisco craton with low $^{87}Sr/^{86}Sr$ ratios of ca. 0.7075 were
330 apparently laid down at ≤ 570 Ma (Paula-Santos et al., 2015). However, in that case, local
331 morphotectonic conditions along the margin of the craton were thought to have modified the Sr-
332 isotope composition of the sea, since sedimentation took place in a restricted foreland basin
333 between the San Francisco craton and emerging chains of the Araçuaí orogen. The more radiogenic

334 $^{87}Sr/^{86}Sr$ ratios of the second group in the Sierras de Córdoba are ambiguous and match the seawater
335 compilation at three different ages: mid-Cambrian (ca. 515 Ma), Ediacaran/Cambrian boundary (ca.
336 545 Ma), and mid-Ediacaran (ca. 580 Ma).

337 From consideration of the C-isotopes alone, it could be suggested that the Sierras de Córdoba
338 Metasedimentary Series represents a single period of deposition on one side or other of the Shuram-
339 Wonoka excursion (Fig. 9a) – between ca. 600 and 550 Ma seawater $\delta^{13}C$ were all negative, down
340 to ca. -12‰ (Melezhik et al., 2009) – i.e., either earlier Ediacaran or late Ediacaran/Cambrian.
341 Nevertheless, using the Halverson et al., 2010 seawater trend, the $\delta^{13}C_{PDB}$ values of the less
342 radiogenic group of samples ($\delta^{13}C$ = -1.05 - +3.54‰) are compatible with the early Ediacaran age
343 obtained from the Sr; such a peak of $\delta^{13}C$ values from slightly negative to positive is recognized
344 between 610 and 630 Ma. An early Ediacaran age for the less radiogenic group of marbles is also
345 compatible with the maximum age of sedimentation recorded by the youngest detrital zircon in
346 sample LC-158 (# 51; 710 ± 11 Ma).

347 For the second group, the $\delta^{13}C_{PDB}$ values ($\delta^{13}C$ = +0.73 to +2.03‰) are most compatible with
348 the Ediacaran/Cambrian option, i.e., ca. 545 Ma. In this case the older, mid-Ediacaran, option can
349 be rejected as at this time $\delta^{13}C$ values should be all negative (coincident with the Shuram-Wonoka
350 excursion). Variations of $\delta^{13}C$ have however been recorded in the mid Ediacaran between ca. 600
351 and 550 Ma (Verdel et al., 2011; An et al., 2015). However all the $\delta^{13}C$ values found in the more
352 radiogenic group of rocks of the Sierras de Córdoba Metasedimentary Series are slightly negative to
353 positive, never strongly negative. Thus we should have to invoke an intervening period of slightly
354 negative to positive $\delta^{13}C$ values during the Shuram-Wonoka period. This possibility remains true on
355 the basis of C-isotope values only. However the Sr-isotope values are against this possibility
356 because they are much higher than those typical of the Mid Ediacaran. We remind here that the Sr-
357 isotope data obtained in this work are remarkably homogeneous and concentrated into two distinct

ages on both sides of the Shuram-Wonoka event. The coincidence of the Sr-isotope composition with that of the C-isotope composition in our rocks makes our interpretation the more realistic. The middle Cambrian option is more difficult to reject on the basis of Sr- and C-isotope compositions alone, but the fact that the peak of regional metamorphism in the Sierras de Córdoba took place in the early Cambrian at 525 – 530 Ma (see below) argues in favour of the second option, i.e., sedimentation close to the Ediacaran/Cambrian boundary.

We propose that the two groups of marbles represent two different ages of sedimentation. The inference is that marbles in the Sierras de Córdoba are part of an original sedimentary succession including siliciclastic and marine limestones that probably extends in time from the early Ediacaran to near the Cambrian/Ediacaran boundary. The possibility of basin restrictions that could produce local isotope composition deviations relative to the open sea is difficult to disprove and therefore our stratigraphic interpretation remains open to question. However, recent paleogeographic models for deposition of the isotopically equivalent Ancajan - Difunta Correa metasedimentary sequences of the Western Sierras Pampeanas, based on detrital zircon ages and Hf-isotope compositions (see below), suggest that the sedimentary basin was an open platform along the margin of a large continental block (e.g, Rapela et al. 2016).

8.2- Stratigraphic correlations

Murra et al. (2011) obtained Sr- and C-isotope compositions for marbles from the sierras of Ancasti and Ancajáan (Fig. 1) where they are abundant (and were long quarried). Two populations of Sr-isotope ratios were recognized (at ca. 0.7076 and ca. 0.7085) that were interpreted as evidence for sedimentation at ~ 570-590 Ma according to the compilation of seawater isotope composition for the late Neoproterozoic and the Cambrian available at that time (Jacobsen and Kaufman, 1999). In fact it is now clear that the two populations are indistinguishable from those found in marbles

382 from the Sierras de Córdoba. Accordingly they are re-interpreted according to the trends of Fig. 9a
383 as stratigraphically correlative with the two groups of marbles identified here.

384 In the western Sierras Pampeanas, marbles in the Difunta Correa Sedimentary Sequence,
385 Sierra de Pie de Palo (Galindo et al., 2004) and the Tambillo Unit, Sierra de Umango (Varela et al.,
386 2001) have $^{87}Sr/^{86}Sr$ ratios comparable with those of the Ediacaran group from the Sierras de
387 Córdoba (mostly 0.7073–0.7075) with mostly positive $\delta^{13}C$ values, albeit up to +12. In consequence
388 the Sierras de Córdoba marbles and those west of it as far as the Andean Cordillera Frontal can
389 probably be stratigraphically correlated.

390 Limestones of the Las Tienditas Formation, representing a subtidal-supratidal environment
391 and contemporary with the upper levels of the Puncoviscana Formation (Omarini et al., 1999) have
392 $^{87}Sr/^{86}Sr$ ratios higher than those of the Sierras de Córdoba and Ancasti (Sial et al., 2001; Lopez de
393 Azarevich et al., 2010) suggesting a younger sedimentation age and/or post-sedimentary alteration
394 as inferred from the high Mg/Ca and Mn/Sr relations. Ages younger than early Cambrian are also
395 indicate by the Sr-isotope compositions of limestones in the Caucete Group, Sierra de Pie de Palo
396 (Galindo et al., 2004) and the Argentine Precordillera (Thomas et al., 2001).

397 Detailed comparison with carbonates of alleged Ediacaran age outside the realm of the early
398 Cambrian Pampean orogenic belt is beyond the scope of this contribution but requires some
399 comment. The Arroyo del Soldado Group is probably one of the most thoroughly studied such
400 successions: isotope information including C, Sr, Nd and Cr, along with palaeontology and accurate
401 lithological descriptions have been presented by Gaucher et al. (2009) and Frei et al. (2011, and
402 references therein). These authors conclude that deposition was late Ediacaran, although some of
403 the Sr-isotope data (e.g., the Polanco Formation) do not match the Halverson et al. (2010) or
404 Kuznetsov et al. (2013) seawater curves for this age. In contrast, Aubet et al. (2012, 2014) conclude
405 that the Arroyo del Soldado Group may be as old as 700 Ma; the cross-cutting Sobresaliente granite

406 has recently been dated at 585 ± 2 Ma (Oyhantçabal et al., 2012). Sánchez Bettucci et al. (2010)
407 were also very critical of the proposed chronology, stratigraphy and tectonic setting of the Arroyo
408 del Soldado Group. Further south along the margin of the Río de la Plata craton, Rapela et al.
409 (2011) argue for a pre-580 Ma sedimentation of the Sierras Bayas Group on the basis of detrital
410 zircon chronology. Sr-isotope composition data (Gómez Peral et al. (2007) were not chemically
411 screened and show moderate Sr contents (<500 ppm) and high Mg/Ca and Mn/Sr ratios, suggesting
412 post-depositional alteration. Further comparison with the Sierras de Córdoba marbles would seem
413 to be premature.
414
415 *8.3- Constraints from U-Pb zircon ages*
416 The younger group of U-Pb ages in sample LC-158, nine of which give a weighted mean age
417 of 527 ± 2 Ma, are from unzoned or complex sector-zoned zircons with low Th (<20 ppm) and
418 Th/U (0.05 and less), strongly suggesting metamorphic growth. It is reasonable to assume that this
419 closely approximates to the time of high-grade metamorphism, since it closely corresponds to the
420 peak of the Pampean orogeny (Rapela et al., 1998b; Escayola et al., 2011). The single peak at 1190
421 Ma in the detrital zircon age pattern (Fig. 8b) implies middle to late Mesoproterozoic sources, but
422 there are also some grains with ages of 1250–1660 Ma on one side of the main peak and 700–1050
423 Ma on the other. This pattern shows many similarities with those of detrital rocks from the Western
424 Sierras Pampeanas interbedded with the Ediacaran marbles discussed above, i.e, the Difunta Correa
425 Sedimentary Sequence and the Ancaján series (Cf. Fig. 7b from Rapela et al., 2016). Comparable
426 patterns have also been reported for some rocks from north-western Argentina (e.g., sample
427 PMXX2 in Adams et al., 2011). Most of the 770–1330 Ma zircon provenance can be explained by
428 derivation from middle to late Mesoproterozoic basement exposed in the Western Sierras
429 Pampeanas, where there are ca. 1070–1330 Ma igneous rocks as well as early Neoproterozoic A-

type granitoids of ca. 770 and 850 Ma (Casquet et al., 2012; and references therein). However, zircon ages of ca. 1330–1560 Ma must reflect sources elsewhere: using Hf-isotope data for zircons of these ages, Rapela et al. (2016) argued in favour of sources in the Southern Granite-Rhyolite Province of southwestern Laurentia (1.3-1.5 Ga; Goodge et al., 2004; 2010). This idea was strengthened by Ramacciotti et al. (2015) with more complete detrital zircon evidence and Nd-isotope composition from the Difunta Correa Sedimentary Sequence, and they further invoked the Mazatzal Province of southwestern Laurentia as the source of a few grains at ca. 1.65 Ga. The scattered Paleoproterozoic detrital zircon ages of ca. 1950–2060 Ma in sample LC-158 were not recorded in either of these studies and their source is unknown.

The detrital zircon age pattern of Fig. 8b differs from that of the pre-Pampean Puncoviscana Formation of northwestern Argentina (defined as above) and equivalents of northern Sierra Chica and Sierra Norte de Córdoba (Adams et al., 2008, 2011; Escayola et al., 2007; Rapela et al., 2007, 2016). There the pattern is strongly bimodal with peaks at ca. 600 and ca. 1000 Ma, with the youngest detrital zircons at 555–570 Ma; interbedded tuffs in the upper part of the series are ca. 537 Ma (Escayola et al., 2011). This pattern is indicative of regional sources in SW Gondwana (e.g., Rapela et al., 2016 and references therein; and more recently Kristoffersen et al., 2016).

8.4- Tectonic implications

Marbles in the Sierras de Córdoba were laid down between the early Ediacaran and the very early Cambrian, apparently in two separate episodes, and are interbedded with siliciclastic rocks with a detrital zircon pattern similar to those of other marble-bearing series to the west (Ancaján series and the Difunta Correa Sedimentary Sequence in the Western Sierras Pampeanas). They differ in these respects from the Puncoviscan Series and the Las Tienditas limestones, strengthening the idea that the Sierras de Córdoba Metasedimentary Series are unrelated to them. Instead they

454 appear to be an extension of the marble-bearing series in the west, implying that the Grenvillian
455 basement of the Western Sierras Pampeanas probably extended beneath them as well and that a
456 tectonic contact must exist somewhere between the latter area and the northern Sierra Chica and
457 Sierra Grande, where the metasedimentary Puncoviscan Series is widespread. The Sierras de
458 Córdoba Metasedimentary Series was involved in the Pampean orogeny at middle crustal levels, in
459 contrast to the sierras to the west (Ancaján, Ancasti and the Western Sierras Pampeanas) where no
460 evidence of significant Pampean metamorphism has been recognized so far. Our work further
461 shows that the Sierras de Córdoba Metasedimentary Series underwent high-grade metamorphism at
462 527 ± 2 Ma (Fig. 8a); a previous U-Pb SHRIMP monazite age of 522 ± 8 Ma for a gneiss sample
463 (Rapela et al., 1998b) is within error of this. Metamorphism was accompanied by folding and
464 ductile shearing in the middle crust. Marbles and meta-siliciclastic rocks of the Sierras de Córdoba
465 were overprinted by major shear zones (e.g., Martino, 2003) that were folded and/or imbricated,
466 resulting in repetition on a W–E cross-section. A dismembered mafic to ultramafic igneous complex
467 is also located in the same shear zones (Bonalumi and Gigena, 1987). This complex has been
468 interpreted as an ophiolitic remnant embracing crustal tracts with oceanic-ridge and probably back-
469 arc chemistry that were tectonically emplaced in a suture (e.g., Ramos et al., 2000), although the
470 age of the mafic–ultramafic complex remains poorly constrained. Our results are compatible with
471 the existence of a strongly reworked suture in the Sierras de Córdoba separating the Ediacaran to
472 early Cambrian cover sequence and its basement in the west from the metasedimentary Puncoviscan
473 Series in the east. The former sedimentary cover would have been part of the lower colliding plate,
474 since Pampean magmatic rocks were emplaced in the Puncoviscana Formation (Rapela et al.,
475 1998b). The Pampean orogeny concluded the amalgamation of SW Gondwana (Rapela et al., 2007)
476 (Fig. 10).

The existence of the Puncoviscana Formation in the Sierra de Ancasti (Toselli et al., 2005; Rapela et al., 2007) separated from the Ancaján series in the eastern part of the mountain range by a strongly deformed zone of Famatinian age, opens the question of the extent of the Pampean suture west of Sierras de Córdoba.

8.5- Paleogeographic hypothesis

Casquet et al. (2012) proposed that the Western Sierras Pampeanas Paleoproterozoic to Mesoproterozoic basement was part of a single large continental block (the MARA block) along the western margin of the Clymene/Puncoviscan ocean (Trindade et al., 2006; Rapela et al., 2016) in Neoproterozoic times. The block was juxtaposed to Laurentia until the early Cambrian when the latter rifted away and the Iapetus Ocean opened. The marble-bearing Difunta Correa Sedimentary Sequence and the Ancaján Series were laid down on this western margin, which collided with the eastern margin during the Pampean orogeny after early Cambrian closure of the Clymene/Puncoviscana ocean. This interpretation has been recently strengthened with more geochronological and Hf-isotope data from detrital zircons (Ramacciotti et al, 2015; Rapela et al., 2016).

We suggest here that the Sierras de Córdoba Metasedimentary Series was laid down on the continental margin of MARA in a more external position than the Ancaján and the Difunta Correa series. Therefore, it was thoroughly involved in the Pampean collisional orogeny whilst the Ancaján and the Difunta Correa rocks remained in the external part of the orogen or in its foreland where penetrative deformation and metamorphism were minor or absent.

9. Conclusions

500 The Sierras de Córdoba Metasedimentary Series consists of marbles of early Ediacaran and
501 early Cambrian age and metasiliciclastic rocks that underwent high-grade metamorphism between
502 525 and 530 Ma during the collisional Pampean orogeny.
503 The Sierras de Córdoba Metasedimentary Series can be correlated on the basis of Sr-isotope
504 evidence from marbles and U-Pb detrital zircon geochronology with other marble-bearing
505 metasedimentary series in several sierras to the west of Sierras de Córdoba (e.g., the Difunta Correa
506 Sedimentary Sequence and the Ancaján Series). All were parts of a former sedimentary cover to the
507 hypothetical MARA block and were laid down on the western margin of the Clymene/Puncoviscan
508 ocean. The Sierras de Córdoba Metasedimentary Series strongly differs (in terms of the age of
509 limestones/marbles and detrital zircon patterns) from the Puncoviscana Formation equivalents of
510 northern Sierra Chica and Sierra Norte and northwestern Argentina. The latter are best interpreted
511 as laid down on the late Ediacaran to early Cambrian eastern margin of the same ocean, with
512 sedimentary input from Gondwana.
513 The Sierras de Córdoba Series and the Puncoviscana Formation (and its equivalents) were
514 probably juxtaposed during the Pampean orogeny along a complex suture zone that was further
515 folded and/or imbricated at middle crust depths. The suture has been inferred from structural
516 evidence and supposed ophiolite remnants (Ramos et al., 2000).
517

518 **Acknowledgements**

519 Financial support for this paper was provided by Argentine public grants SECYT-UNC 2014/2015
520 05/I768, FONCYT PICT 2013-0472, CONICET PIP 0229 and Spanish grants CGL2009-07984 and
521 GR58/08 UCM-Santander. We acknowledge Dr. F. Tornos (Centro de Astrobiología, Madrid) and
522 Dr. C. Recio (Salamanca University) for the stable isotope work. Ms. B. Soutullo (UCM) helped
523 with some of the XRD determinations. This contribution has benefited from comments from Drs.

524 Eben Hodgin and Paulo Boggiani, and two anonymous reviewers who helped us to improve the
525 manuscript.

526

527 **References**

528 Adams, C., Miller, H., Toselli, A.J., Griffin,W.L., 2008. The Puncoviscana Formation of northwest
529 Argentina: U–Pb geochronology of detrital zircons and Rb–Sr metamorphic ages and their
530 bearing on its stratigraphic age, sediment provenance and tectonic setting. Neues Jahrbuch für
531 Geologie und Paläontologie Abhandlungen 247, 341–352.

532 Adams, C.J., Miller, H., Aceñolaza, F.G., Toselli, A.J., Griffin,W.L., 2011. The Pacific Gondwana
533 margin in the late Neoproterozoic–early Paleozoic: detrital zircon U–Pb ages from
534 metasediments in northwest Argentina reveal their maximum age, provenance and tectonic
535 setting. Gondwana Research 19 (1), 71–83.

536 An, Z., Jiang, G., Tong, J., Tian, L., Ye, Q., Song, H., Song, H., 2015. Stratigraphic position of the
537 Ediacaran Miaohe biota and its constrains on the age of the upper Doushantuo $\delta^{13}C$ anomaly
538 in the Yangtze Gorges area, South China. Precambrian Research, 271, 243-253.

539 Aubet, N., Pecoits, E., Bekker, A., Gingras, M., Zwingmann, H, Veroslavsky, G., de Santa Ana, H.,
540 Konhauser, K., 2012. Chemostratigraphic constraints on early Ediacaran carbonate ramp
541 dynamics, Río de la Plata craton, Uruguay. Gondwana Research 22 (3-4), 1073–1090.

542 Aubet, N., Pecoits, E., Heaman, L., Veroslavsky, G., Gingras, M., Konhauser, K., 2014. Ediacaran
543 in Uruguay: Facts and controversies. Journal of South American Earth Sciences 55, 43-57.

544 Babinski, M., Boggiani, P. C., Fanning, M., Simon, C. M., Sial, A. N. 2008. U–Pb SHRIMP
545 geochronology and isotope chemostratigraphy (C, O, Sr) of the Tamengo Formation, southern
546 Paraguay belt, Brazil. In: South American Symposium on Isotope Geology, 6, San Carlos de
547 Bariloche, Argentina. Proceedings, CD-ROM.

548 Baldo, E.G., 1992. Estudio petrológico y geoquímico de las rocas ígneas y metamórficas entre
549 Pampa de Olaen y Characato, extremo norte de las Sierras Grandes de Córdoba, Córdoba,
550 República Argentina. PhD, School Newspaper of Exact, Physical and Natural Sciences,
551 National University of Córdoba, 305 p. (unpublished).
552 Baldo, E., Casquet C., Galindo, C., 1996. El metamorfismo de la Sierra Chica de Córdoba (Sierras
553 Pampeanas). Argentina. Geogaceta 19, 51–54.
554 Baldo, E., Rapela, C.W., Pankhurst, R.J., Galindo, C., Casquet, C., Verdecchia, S., Murra, J., 2014.
555 Geocronología de las Sierras de Córdoba: revisión y comentarios. In: Relatorio del XIX
556 Congreso Geológico Argentino: Geología y Recursos Naturales de la Provincia De Córdoba
557 (Martino, R., Guereschi, A., Eds.) 845-868.
558 Bonalumi, A.A., Gigena, A.A., 1987. Relación entre las metamorfitas de alto grado y las rocas
559 básicas y ultrabásicas en el Dpto. Calamuchita, Córdoba. Revista de la Asociación Geológica
560 Argentina 42(1-2), 73-81.
561 Bonalumi, A., Escayola, M., Kraemer, P., Baldo E., Martino, R., 1999. Sierras Pampeanas
562 (Córdoba, Santiago del Estero). A) Precámbrico-Paleozoico inferior de las Sierras de
563 Córdoba. In: Caminos, R. (Ed.) Geología Argentina. Instituto de Geología y Recursos
564 Minerales. Buenos Aires. Anales 29, 136–140.
565 Brand, U., Veizer, J., 1980. Chemical diagenesis of a multicomponent carbonate system – 1: Trace
566 elements. Journal of Sedimentary Petrology 50 (4), 1219–1236.
567 Burke, W. H., Denison, R. E., Hetherington, E. A., Koepnick, R. B., Nelson, H. F., Otto, J. B.,
568 1982. Variation of seawater $^{87}Sr/^{86}Sr$ throughout Phanerozoic time. Geology 10 (10), 516-519.
569 Casquet, C., Rapela, C., Pankhurst, R., Galindo, C., Dahlquist, J., Baldo, E., Saavedra, J., González
570 Casado, J., Fanning, M., 2004. Grenvillian massif-type anorthosites in the Sierras Pampeanas.
571 Journal of Geological Society 162, 9-12.

572 Casquet, C., Pankhurst, R., Rapela, C., Galindo, C., Fanning, C., Chiaradia, M., Baldo, E.,
573 González-Casado, J., Dahlquist, J., 2008. The Mesoproterozoic Maz terrane in the Western
574 Sierras Pampeanas, Argentina, equivalent to the Arequipa-Antofalla block of southern Peru?
575 Implications for West Gondwana margin evolution. Gondwana Research 13 (2), 163-175.
576 Casquet, C., Rapela, C.W., Pankhurst, R.J., Baldo, E.G., Galindo, C., Fanning, C.M., Dahlquist,
577 J.A., Saavedra, J., 2012. A history of Proterozoic terranes in southern South America: From
578 Rodinia to Gondwana. Geoscience Frontiers 3(2), 137-145.
579 Casquet, C., Rapela, C.W., Baldo, E., Pankhurst, R., Galindo, C., Verdecchia, S., Murra, J.,
580 Dahlquist, J., 2014. The relationships between pre- and syn-Pampean orogeny
581 metasedimentary rocks in the Eastern Sierras Pampeanas. In: "Gondwana 15 Symposium",
582 Abstracts book, 29 (http://eprints.ucm.es/26351/) Madrid, España (Spain).
583 Costa, C., Gardini, C., Chiesa, J., Ortiz Suárez, A., Ojeda, G., Rivarola, D., Tognelli, G., Strasser,
584 E., Carugno Durán, A., Morla, P., Guerstein, P., 2001. Hoja Geológica 3366-III, San Luis,
585 provincias de San Luis y Mendoza. SEGEMAR, Boletín 293, in CD.
586 Craig, H., 1957. Isotopic standards for carbon and oxygen and correction factors for mass-
587 spectrometric analysis of carbon dioxide. Geochimica Cosmochimica Acta 12 (1-2), 133-
588 149.
589 Dahlquist, J.A., Pankhurst, R.J., Rapela, C.W., Galindo, C., Alasino, P., Fanning, C.M., Saavedra,
590 J., Baldo, E., 2008. New SHRIMP U–Pb data from the Famatina Complex: constraining
591 early–mid Ordovician Famatinian magmatism in the Sierras Pampeanas, Argentina.
592 Geologica Acta 6 (4), 319–333.
593 Derry, L.A., Keto, L.S., Jacobsen, S.B., Knoll, A.H., Swett, K., 1989. Strontium isotopic variations
594 in Upper Proterozoic carbonates from Svalbard and East Greenland. Geochim. Cosmochim
595 Acta 53, 2331-2339.

596 Derry, L.A., Kaufman, A.J., Jacobsen, S.B., 1992. Sedimentary cycling and environmental change
597 in the Late Proterozoic: Evidence from stable and radiogenic isotopes. Geochim. Cosmochim.
598 Acta 56 (3), 1317–1329.
599 Do Campo, M., Ribeiro Guevara, S., 2005. Provenance analysis and tectonic setting of late
600 Neoproterozoic metasedimentary successions in NW Argentina. Journal of South American
601 Earth Sciences, 19 (2), 143-153.
602 Escayola, M.P., Pimentel, M.M., Armstrong, R., 2007. Neoproterozoic backarc basin: sensitive
603 high-resolution ion microprobe U–Pb and Sm–Nd isotopic evidence from the Eastern
604 Pampean Ranges, Argentina. Geology 35 (6), 495–498.
605 Escayola, M.P., van Staal, C.R., Davis, W.J., 2011. The age and tectonic setting of the
606 Puncoviscana Formation in northwestern Argentina: An accretionary complex related to early
607 Cambrian closure of the Puncoviscana Ocean and accretion of the Arequipa– Antofalla block.
608 Journal of South American Earth Sciences 32 (4), 438–459.
609 Fairchild, I., Marshall, J., Bertrand-Sarafati, J., 1990. Stratigraphic shifts in carbon isotopes from
610 Proterozoic stromatolitic carbonates (Mauritania): influences of primary mineralogy and
611 diagenesis. American Journal of Science, 290-A, 46–79.
612 Frei, R., Gaucher, C., Døssing, L.N., Sial, A.N., 2011. Chromium isotopes in carbonates – A tracer
613 for climate change and for reconstructing the redox state of ancient seawater. Earth and
614 Planetary Science Letters 312 (1-2), 114-125.
615 Fuenlabrada, J.M., Galindo, C., 2001. Comportamiento de la relación 87Sr/86Sr en disoluciones de
616 carbonatos impuros en función de la concentración ácida y en disoluciones de sulfatos en
617 función del tiempo. Actas III Congreso Ibérico de Geología, 591-595.
618 Galindo, C., Casquet, C., Rapela, C., Pankhurst, R.J., Baldo, E., Saavedra, J., 2004. Sr, C and O
619 isotope geochemistry and stratigraphy of Precambrian and lower Paleozoic carbonate

620 sequences from the Western Sierras Pampeanas of Argentina: tectonic implications.
621 Precambrian Research 131, 55–71.
622 Gaucher, C., Sial, A.N., Poiré, D., Gómez-Peral, L., Ferreira, V.P., Pimentel, M.M., 2009.
623 Chemostratigraphy. Neoproterozoic-Cambrian evolution of the Río de la Plata
624 Palaeocontinent. In: Gaucher, C., Sial, A.N., Halverson, G.P., Frimmel, H.E. (Eds.):
625 Neoproterozoic-Cambrian tectonics, global change and evolution: a focus on southwestern
626 Gondwana. Developments in Precambrian Geology, 16, Elsevier, pp. 115-122.
627 Gómez Peral, L.E., Poiré, D.G., Strauss, H., Zimmermann, U., 2007. Chemostratigraphy
628 and diagenetic constraints on Neoproterozoic carbonate successions from the Sierras
629 Bayas Group, Tandilia System, Argentina. Chemical Geology 237 (1-2), 109-128.
630 Goodge, J.W., Williams, I.S., Myrow, P., 2004. Provenance of Neoproterozoic and lower Paleozoic
631 siliciclastic rocks of the central Ross orogen, Antarctica: Detrital record of rift-, passive-, and
632 active-margin sedimentation. Geological Society of America Bulletin 116 (9.10), 1253-1279.
633 Goodge, J.W., Fanning, C.M., Brecke, D.M., Licht, K.J., Palmer, E.F., 2010. Continuation of the
634 Laurentian Grenville Province across the Ross Sea Margin of East Antarctica. The Journal of
635 Geology 118, 601–619.
636 Gordillo, C., 1984. Migmatitas cordieríticas de la Sierras de Córdoba; condiciones físicas de la
637 migmatización. Boletín de la Academia Nacional de Ciencias 68, 3–40.
638 Gordillo, C., Lencinas, A., 1979. Sierras Pampeanas de Córdoba y San Luis. Segundo Simposio de
639 Geología Regional Argentina. Academia Nacional de Ciencias, Córdoba, I, 577–650.
640 Gordillo, C., Bonalumi, A. 1987. Termobarometría de la faja migmática de “La Puerta,
641 Departamento Cruz del Eje, Provincia de Córdoba. Revista de la Asociación Geológica
642 Argentina 42(3-4), 255–266.

643 Guereschi, A., Martino, R., 2002. Geotermobarometría de la paragénesis Qtz + Pl + Bt + Grt + Sil
644 en gneises del sector centro-oriental de la sierra de Comechingones, Córdoba. Revista de la
645 Asociación Geológica Argentina 57 (4), 365-375.
646 Guereschi, A., Martino, R., 2003. Trayectoria textural de las metamorfitas del sector centro-oriental
647 de la sierra de Comechingones, Córdoba. Revista de la Asociación Geológica Argentina
648 58(1), 61–77.
649 Halverson, G.P., Dudás, F.Ö., Maloof, A.S., Bowring, S.A., 2007. Evolution of $^{87}Sr/^{86}Sr$
650 composition of Neoproterozoic seawater. Palaeogeography, Palaeoclimatology,
651 Palaeoecology 256 (3-4), 103–129.
652 Halverson, G.P., Wade, B.P., Hurtgen, M.T., Barovich, K.M., 2010. Neoproterozoic
653 chemostratigraphy. Precambrian Research 182 (4), 337–350.
654 Harley, S.L., Kelly, N.M., Möller, A. 2007, Zircon behaviour and the thermal histories of mountain
655 chains. Elements 3 (1), 25-30.
656 Iannizzotto, N.F., Rapela, C.W., Baldo, E.G., 2011. Nuevos datos geocronológicos, geoquímicos e
657 isotópicos del Batolito de Sierra Norte-Ambargasta en su sector más austral, Provincia de
658 Córdoba. 18º Congreso Geológico Argentino, Actas del Simposio de Tectónica Pre-Andina
659 (S2), 190–191. Neuquén.
660 Jacobsen, S.B., Kaufman, A.J., 1999. The Sr, C and O isotopic evolution of Neoproterozoic
661 seawater. Chemical Geology 161 (1-3), 37–57.
662 Jiang, G., Kaufman, A., Christie-Blick, N., Zhang, S., Wu, H., 2007. Carbon isotope variability
663 across the Ediacaran Yangtze platform in South China: Implications for a large surface-to-
664 deep ocean $\delta^{13}C$ gradient. Earth and Planetary Science Letters 261 (1-2), 303–320.

665 Kristoffersen, M., Andersen, T., Elburg, M.A., Watkeys, M.K., 2015. Detrital zircon in a
666 supercontinental setting: locally derived and far-transported components in the Ordovician
667 Natal Group, South Africa. Journal of the Geological Society 173 (1), 203-215.
668 Kuznetsov, A.B., 1998. Evolution of Sr isotopic composition in late Riphean seawater: the Karatau
669 Group carbonates, Southern Urals. Unpub. Ph.D. Thesis, St. Petersburg, Institute of
670 Precambrian Geology and Geochronology, Russian Academy of Sciences, Russia, p. 190, (in
671 Russian).
672 Kuznetsov, A.B., Ovchinnikova, G.V., Gorokhov, I.M., Letnikova, E.F., Kaurova, O.K,
673 Konstantinova, G.V., 2013. Age constraints on the Neoproterozoic Baikal Group from
674 combined Sr isotopes and Pb–Pb dating of carbonates from the Baikal type section,
675 southeastern Siberia. Journal of Asian Earth Sciences 62, 51–66.
676 Letnikova, E.F., Kuznetsov, A.B., Vishnevskaya, I.A., Terleev, A.A., Konstantinova, G.V., 2011.
677 The geochemical and isotope (Sr, C, O) characteristics of the Vendian- Cambrian carbonate
678 deposits of the Azyr-Tal Ridge (*Kuznetsk Alatau*): chemostratigraphy and sedimentogenesis
679 environments. Russian Geology and Geophysics, 52, 1154-1170.
680 Lira, R., Sfragulla, J., 2014. El magmatismo Devónico-Carbonífero: El batolito de Achala y
681 plutones menores al norte del cerro Champaquí. In: Relatorio del XIX Congreso Geológico
682 Argentino: Geología y Recursos Naturales de la Provincia de Córdoba (Martino, R.,
683 Guereschi, A., (Eds.) 293-347.
684 López de Azarevich, V., Omarini, R., Santos, R., Azarevich, M., Sureda, R., 2010. Nuevos aportes
685 isotópicos para secuencias carbonáticas del Precámbrico superior (Formación Las Tienditas)
686 del NO de Argentina: su implicancia en la evolución de la Cuenca Puncoviscana. Serie
687 Correlación Geológica 26, 27-48.

688 Ludwig, K.R., 2003. Isoplot/Ex version 3.0: A geochronological toolkit for Microsoft Excel.
689 Berkeley Geochronology Center Special Publication Nº 4, 2455 Ridge Road, Berkeley *CA*
690 94709, USA.
691 Martino, R., 2003. Las fajas de deformación dúctil de las Sierras Pampeanas de Córdoba: Una
692 reseña general. Revista Asociación Geológica Argentina 58 (4), 549-571.
693 McCrea, J.M., 1950. On the isotopic chemistry of carbonates and a paleotemperature scale. The
694 Journal of Chemical Physics 18 (6), 849-857.
695 Melezhik, V.A., Gorokhov, I.M., Fallick, A.E., Gjelle, S., 2001. Strontium and carbon isotope
696 geochemistry applied to dating of carbonate sedimentation: an example from high-grade rocks
697 of the Norwegian Caledonides. Precambrian Research108 (3-4), 267–292.
698 Melezhik, V., Pokrovsky, B., Fallick, A., Kuznetsov, A., Bujakaite, M., 2009. Constraints on
699 $^{87}Sr/^{86}Sr$ of Late Ediacaran seawater: insight from Siberian high-Sr limestones. Journal of the
700 Geological Society, London 166, 183–191.
701 Montañez, I., Osleger, D., Banner, J., Mack, L., Musgrove, M., 2000. Evolution of the Sr and C
702 isotope composition of Cambrian oceans. Geological Society of America Today 10(5), 1-5.
703 Montero, P., Haissen, F., El Archi, A., Rjimati, E., Bea, F., 2014. Timing of Archean crust
704 formation and cratonization in the Awsard-Tichla zone of the NW Reguibat Rise, West
705 African Craton: A SHRIMP, Nd–Sr isotopes, and geochemical reconnaissance study.
706 Precambrian Research 242, 112-137.
707 Murra, J.A., Baldo, E.G., Galindo, C., Casquet, C., Pankhurst, R.J., Rapela, C.W., Dahlquist, J.,
708 2011. Sr, C and O isotope composition of marbles from the Sierra de Ancasti, Eastern Sierras

709 Pampeanas, Argentina: age and constraints for the Neoproterozoic–Lower Paleozoic
710 evolution of the proto-Gondwana margin. Geologica Acta 9, 79–92.
711 Omarini, R., Sureda, R., Götze, H., Seilacher, A., Pflüger, F., 1999. Puncoviscana folded belt in
712 northwestern Argentina: testimony of Late Proterozoic Rodinia fragmentation and pre-
713 Gondwana collisional episodes. International Journal of Earth Sciences, 88 (1), 76-97.
714 Oyhantçabal, P., Wagner-Eimer, M., Wemmer, K., Schulz, B., Frei, R., Siegesmund, S., 2012.
715 Paleo- and Neoproterozoic magmatic and tectonometamorphic evolution of the Isla Cristalina
716 de Rivera (Nico Pérez Terrane, Uruguay). Int. J. Earth Sci. (Geol. Rundsch.) 101 (7), 1745–
717 1762.
718 Pankhurst, R.J., Rapela, C.W., 1998. The Proto-Andean margin of Gondwana: an introduction. In:
719 Pankhurst, R.J., Rapela, C.W. (Eds.), The Proto-Andean Margin of Gondwana. Geological
720 Society, London, Special Publications 142, pp. 1–9.
721 Paula-Santos, G. M., Babinski, M., Kuchenbecker, M., Caetano-Filho, S., Trindade, R. I., Pedrosa-
722 Soares, A. C. 2015. New evidence of an Ediacaran age for the Bambuí Group in southern São
723 Francisco craton (eastern Brazil) from zircon U–Pb data and isotope chemostratigraphy.
724 Gondwana Research 28 (2), 702-720.
725 Prokoph, A., Shields, G., Veizer, J., 2008. Compilation and time-series analysis of a marine
726 carbonate $\delta^{18}O$, $\delta^{13}C$, $^{87}Sr/^{86}Sr$ and $\delta^{34}S$ database through Earth history. Earth-Science
727 Reviews 87 (3-4), 113–133.
728 Ramacciotti, C.D., Baldo, E.G., Casquet, C., 2015. U-Pb SHRIMP detrital zircon ages from the
729 Neoproterozoic Difunta Correa Metasedimentary Sequence (Western Sierras Pampeanas,
730 Argentina): Provenance and paleogeographic implications. Precambrian Research 270, 39-49.
731 Ramos, V., Escayola, M., Mutti, D. y Vujovich, G., 2000. Proterozoic-early Paleozoic ophiolites in
732 the Andean basement of southern South America. In: Dilek, Y., Moores, E., Elthon, D. y

733 Nicolas, A. (Eds.), Ophiolites and oceanic crust: new insights from field studies and ocean
734 drilling program. Geological Society of America, Special paper, 349: 331-349.
735 Ramos, V.A., Vujovich, G., Martino, R., Otamendi, J., 2010. Pampia: a large cratonic block missing
736 in the Rodinia supercontinent. Journal of Geodynamics 50(3-4), 243–255.
737 Rapela, C., Pankhurst, R., Casquet, C., Baldo, E., Saavedra, J., Galindo, C., 1998a. Early evolution
738 of the Proto-Andean margin of South America. Geology 26(8), 707-710.
739 Rapela, C.W., Pankhurst, R.J., Casquet, C., Baldo, E., Saavedra, J., Galindo, C., Fanning, C.M.,
740 1998b. The Pampean orogeny of the southern proto-Andes: Cambrian continental collision in
741 the Sierras de Córdoba. In: Pankhurst, R.J., Rapela, C.W. (Eds.), The Proto-Andean Margin of
742 Gondwana. Geological Society, of London, Special Publication 142, 181–217.
743 Rapela, C.W., Casquet, C., Baldo, E., Dahlquist, J., Pankhurst, R., Galindo, C., Saavedra, J., 2001.
744 Las Orogénesis del Paleozoico Inferior en el margen proto-andino de América del Sur, Sierras
745 Pampeanas, Argentina. Journal of Iberian Geology 27, 23-41.
746 Rapela, C.W., Baldo, E.G., Pankhurst, R.J., Saavedra, J., 2002. Cordieritite and leucogranite
747 formation during emplacement of highly peraluminous magma: the El Pilón Granite Complex
748 (Sierras Pampeanas, Argentina). Journal of Petrology 43 (6), 1003–1028.
749 Rapela, C.W., Pankhurst, R., Casquet, C., Fanning, C., Baldo, E., González-Casado, J., Galindo, C.,
750 Dahlquist, J., 2007. The Río de la Plata craton and the assembly of SW Gondwana. Earth-
751 Science Reviews 83 (1-2), 49-82.
752 Rapela, C.W., Pankhurst, R.J., Casquet, C., Baldo, E., Galindo, C., Fanning, C.M., Dahlquist, J.,
753 2010. The Western Sierras Pampeanas: protracted Grenville-age history (1330-1030 Ma) of
754 intra-oceanic arcs, subduction-accretion at continental-edge and AMCG intraplate
755 magmatism. Journal of South American Earth Sciences 29, 105-127.

Rapela, C.W., Fanning, C.M., Casquet, C., Pankhurst, R.J., Spalletti, L., Poiré, D., Baldo, E.G., 2011, The Rio de la Plata craton and the adjoining Pan-African/brasiliano terranes: Their origins and incorporation into south-west Gondwana. Gondwana Research 20 (4), 673–690.

Rapela, C.W., Verdecchia, S.O., Casquet, C., Pankhurst, R.J., Baldo, E., Galindo, C., Murra, J.A., Dahlquist, J.A., Fanning, M., 2016. Identifying Laurentian and SW Gondwana sources in the Neoproterozoic to early Paleozoic metasedimentary rocks of the Sierras Pampeanas: Paleogeographic and tectonic implications. Gondwana Research 32, 193-212.

Rasband, W.S., ImageJ, U. S. National Institutes of Health, Bethesda, Maryland, USA, http://imagej.nih.gov/ij/, 1997-2015.

Sánchez Bettucci, L., Masquelin, E., Peel, E., Oyhantçabal, P., Muzio, R., Ledesma, J.J., Preciozzi, F., 2010. Comment on "Provenance of the Arroyo del Soldado Group (Ediacaran to Cambrian, Uruguay): implications for the palaeogeographic evolution of southwestern Gondwana" by Blanco et al. [Precambrian Res 171 (2009) 57-73]. Precambrian Research 180 (3-4), 328-333.

Schwartz, J.J., Gromet, L.P., 2004. Provenance of Late Proterozoic–early Cambrian basin, Sierras de Córdoba, Argentina. Precambrian Research 129 (1-2), 1–21.

Schwartz, J.J., Gromet, L.P., Miro, R., 2008. Timing and duration of the calc-alkaline arc of the Pampean orogeny: implications for the Late Neoproterozoic to Cambrian evolution of Western Gondwana. Journal of Geology 116 (1), 39–61.

Sial, A.N., Ferreira, V.P., Aceñolaza, F.G., Pimentel, M.M., Parada, M.A., Alonso, R.N., 2001. C and Sr isotopic evolution of carbonate sequences in NW Argentina: implications for a probable Precambrian-Cambrian transition. Carbonates and Evaporites, 16 (2), 141-152.

Sims, J, Ireland, T., Camacho, A., Lyons, P., Pieters, P., Skirrow, R., Stuart-Smith, P., Miró, R., 1998. U-Pb, Th-Pb and Ar-Ar geochronology from the southern Sierras Pampeanas,

780 Argentina: implications for the Paleozoic tectonic evolution of the western Gondwana margin.
781 In: Pankhurst, R., Rapela, C. (Eds). The proto-Andean Margin of Gondwana. Geological
782 Society, London, Special Publication 142, p. 259-281.
783 Steenken, A., Wemmer, K., Martino, R. D., López De Luchi, M. G., Guereschi, A., Siegesmund, S.,
784 2010. Post-Pampean cooling and the uplift of the Sierras Pampeanas in the west of Córdoba
785 (Central Argentina). N. Jb. Geol. Paläont. Abh. 256 (2), 235-255.
786 Thomas, W., Astini, R., Denison, R., 2001. Strontium Isotopes, Age, and Tectonic Setting of
787 Cambrian Salinas along the Rift and Transform Margins of the Argentine Precordillera and
788 Southern Laurentia. The Journal of Geology 109 (2), 231–246.
789 Toselli, A., Aceñolaza, F., Sial, A., Rossi, J., Ferreira, V., Alonso, R., 2005. Los carbonatos de la
790 Formación Puncoviscana s.l.: correlación quimioestratigráfica e interpretación geológica. XVI
791 Congreso Geológico Argentino 2 (Actas), 327-333.
792 Toselli, A.J., Gaucher, C, Aceñolaza, G.F., Frei, R., Aceñolaza, F.G., Sial, A.N., Rossi, J.N., 2010.
793 New 87Sr/86Sr data on limestones of the Puncoviscana Formation and Sierras Pampeanas of
794 Catamarca, Argentina. VII – South American Symposium on Isotope Geology (VII-SSAGI).
795 Brasilia. Publicación CD-SO440.
796 Toselli, A.J., Aceñolaza, G.F., Miller, H., Adams, C., Aceñolaza, F.G., Rossi, J.N., 2012. Basin
797 evolution of the margin of Gondwana at the Neoproterozoic/Cambrian transition: the
798 Puncoviscana Formation of Northwest Argentina. – N. Jb. Geol. Paläont. Abh. 265, 79-95.
799 Trindade, R., DÁgrella-Filho, M., Epof, I., Brito Neves, B., 2006. Paleomagnetism of early
800 Cambrian Itabaiana mafic dikes (NE Brazil) and the final assembly of Gondwana: Earth and
801 Planetary Science Letters 244 (1-2), 361–377.
802 Varela, R., Valencio, S., Ramos, A., Sato, K., González, P., Panarello, H., Roverano, D., 2001.
803 Isotopic strontium, carbon and oxygen study on Neoproterozoic marbles from Sierra de

804 Umango, Andean foreland, Argentina. III South American Symposium on Isotope Geology,
805 Extended Abstracts, 450-453, Pucón, Chile.
806 Veizer, J., Ala, D., Azmy, K., Bruckschen, P., Buhl, D., Bruhn, F., Carden, G.A.F., Diener, A.,
807 Ebneth, S., Godderis, Y., Jasper, T., Korte, C., Pawellek, F., Podlaha, O.G., y Strauss, H.,
808 1999. $^{87}Sr/^{86}Sr$, $\delta\,^{13}C$ and $\delta\,^{18}O$ evolution of Phanerozoic seawater. Chemical Geology 161 (1-
809 3), 59–88.
810 Verdel, C., Wernicke, B.P., Bowring, S.A., 2011. The Shuram and subsequent Ediacaran carbon
811 isotope excursions from southwest Laurentia, and implications for environmental stability
812 during the metazoan radiation. Geological Society of America Bulletin, 123 (7-8), 1539-1559.
813 von Gosen,W., McClelland,W.C., Loske,W.,Martínez, J.C., Prozzi, C., 2014. Geochronology of
814 igneous rocks in the Sierra Norte de Córdoba (Argentina): implications for the Pampean
815 evolution at the western Gondwana margin. Lithosphere 6 (4), 277–300.
816 Vujovich, G., van Staal, C., Davis, W., 2004. Age constraints on the tectonic evolution and
817 provenance of the Pie de Palo Complex, Cuyania Composite Terrane, and the Famatinian
818 Orogeny in the Sierra de Pie de Palo, San Juan, Argentina. Gondwana Research 7(4), 1041-
819 1056.
820 Whitney, D.L., Evans, B.W., 2010. Abbreviations for names of rock-forming minerals. American
821 Mineralogist 95, 185–187.
822 Williams, I.S., 1998. U–Th–Pb geochronology by ion microprobe. In*:* McKibben, M. A., Shanks
823 III, W.C., Ridley, W.I. (Eds.), Applications of Microanalytical Techniques to Understanding
824 Mineralizing Processes. Reviews in Economic Geology 7, 1–35.
825 Zimmermann, U., 2005. Provenance studies of very low- to low-grade metasedimentary rocks of
826 the Puncoviscana complex, northwest Argentina. In: Vaughan, A.P.M., Leat, P.T., Pankhurst,
827 R.J. (Eds). Geological Society, London, Special Publications 246, 381–416.

828 **Figure Captions:**

829 **Figure 1.** Map of the Sierras Pampeanas (WSP and ESP) and northwestern Argentina. Main
830 ranges abbreviations: Sierra de Ambato (Am), Sierra de Ancasti (An), Sierra de Guasayan (Gu),
831 Sierra de Ancaján (SAn), Sierra del Toro Negro (STN), Sierra de Umango (Um), Sierras de Maz-
832 Espinal (ME), Sierra Brava (SB), Sierra Norte-Ambargasta (SNA), Sierra de Valle Fertil-La Huerta
833 (VFLH), Sierra de Pie de Palo (PP),Sierra del Gigante (dG), Sierra de Córdoba (SC) and Sierra de
834 San Luis (SSL). Modified from Rapela et al. (2016).

835

836 **Figure 2**. Simplified geological map of the Sierras de Córdoba (after Martino, 2003 and
837 Baldo et al., 2014) showing the main bands of marble and calcsilicate rocks. Sampling localities: 1-
838 Quilpo; 2-Centenario; 3-La Falda; 4-El Cuadrado; 5-El Sauce; 6-Dumesnil; 7-Cantesur; 8-La
839 Calera; 9-Las Jarillas; 10-Alta Gracia; 11-San Agustín; 12-Santa Rosa; 13-Sol de Mayo; 14-San
840 Miguel; 15-Santa Mónica; 16-Cañada de Álvarez; 17-Achiras; 18-Lujan; 19-La Suiza; 20-Altautina;
841 21-Tala Cañada; 22-Cuchiyaco; 23-Igam; 24-Characato; 25-Iguazú; 26-Ciénaga del Coro.

842

843 **Figure 3.** a) Pure white marble in contact with amphibolites in the Quilpo quarry, Sierra
844 Chica belt; b) marble with interbedded metapelites near the IGAM quarry, Sierra Grande belt; c)
845 banded marble in the La Suiza quarry, San Luis; d) folded marble in the Dumesnil quarry, Sierra
846 Chica belt.

847

848 **Figure 4.** Close-up view of marble types: a) pure white fine-grained (Quilpo quarry, Sierra
849 Chica belt); b) pure bluish coarse-grained (Characato, Sierra Grande belt); c) grey massive coarse-
850 grained (Iguazu quarry, Sierra Grande belt); d) grey to white banded medium to coarse-grained (La
851 Suiza quarry, San Luis).

852

853 **Figure 5.** a) Migmatite (stromatite) interbedded with marbles, where sample LC-158 was
854 collected; b) outcrop view; c) photomicrograph of LC-158 (PPL) showing irregular garnet grains.
855

856 **Figure 6.** Chemical screening plots of marbles from the Sierras de Córdoba showing the
857 post-depositional alteration boundaries according to Melezhik et al. (2001).
858

859 **Figure 7.** Cathodoluminiscence (CL) images of zircon grains from sample LC-158 showing
860 location of analysed spots and age. a) Detrital elongated igneous grains; b) metamorphic grains. See
861 text for details.
862

863 **Figure 8.** U–Pb zircon results for migmatite gneiss LC-158. (a) Tera-Wasserburg diagram
864 plotted without common Pb-correction (error ellipses are 68% confidence limits); (b) probability
865 density plot of ages of pre-metamorphism detrital grains.
866

867 **Figure 9.** a) $^{87}Sr/^{86}Sr$ ratios and $\delta^{13}C_{PDB}$ composition of Neoproterozoic to the Early
868 Paleozoic seawater carbonates after compilation of Halverson et al. (2010). The Sierras de Córdoba
869 marbles with $^{87}Sr/^{86}Sr$ ratios of 0.7074 – 0.7077 suggest an Ediacaran age of sedimentation while
870 $^{87}Sr/^{86}Sr$ ratios of 0.7083 – 0.7086 suggest an early Cambrian age (see text for discussion). The
871 $\delta^{13}C_{PDB}$ values of Ediacaran marbles further constrain the proximity to the Marinoan glaciation age.
872 b) Updating of the Sierra de Ancasti early marble age by Murra et al. (2011) according to the recent
873 isotope compilation of Halverson et al. (2010).

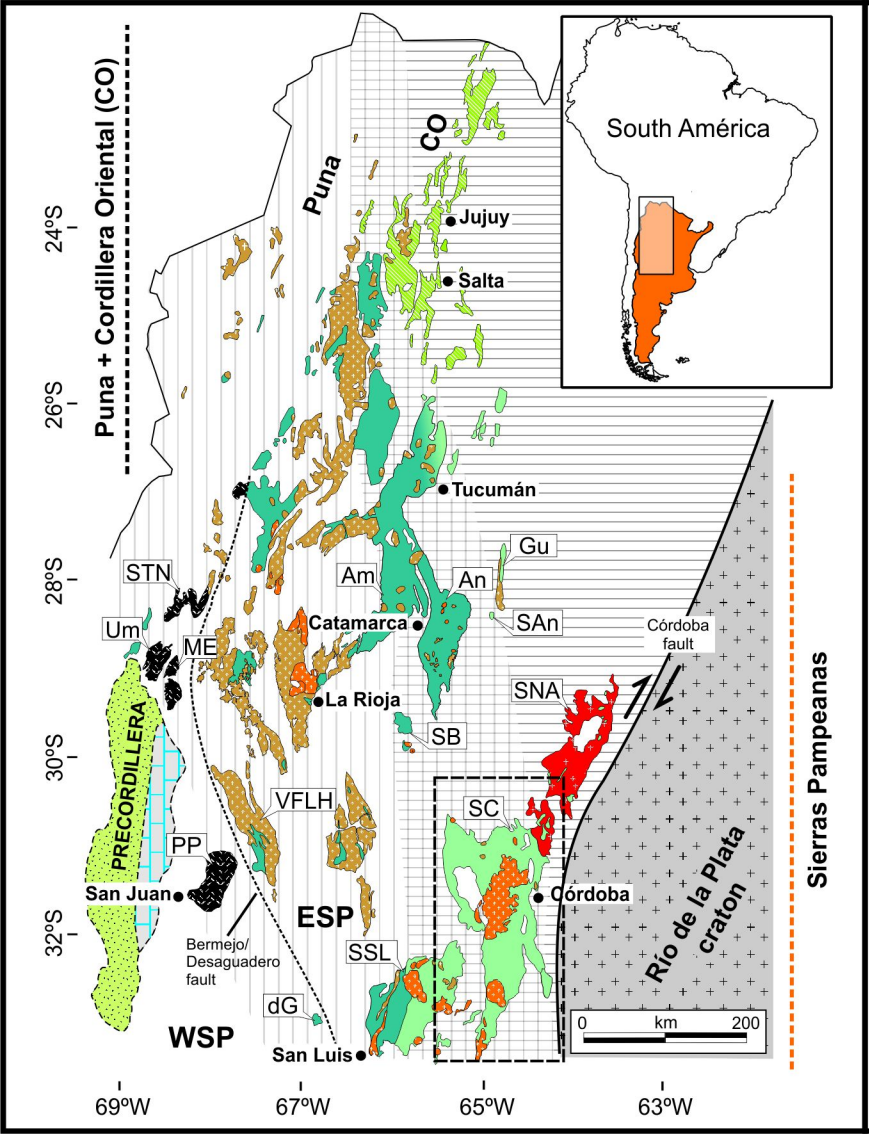

Key

- Devonian to Carboniferous igneous rocks
- Early Ordovician igneous rocks
- Early Ordovician metamorphic rocks
- Ordovician igneous and metamorphic rocks in Mesoproterozoic basement
- Ordovician siliciclastic sequences
- Cambrian to Ordovician carbonate platform
- Cambrian igneous rocks
- Ediacaran to Early Cambrian metasedimentary rocks (Puncoviscana Formation)
- Neoproterozoic to Early Cambrian metamorphic rocks
- Paleoproterozoic basement, Río de La Plata craton (not in outcrop)
- Pampean Orogeny
- Famatinian Orogeny
- Overlapping of Pampean and Famatinian orogenies

WSP Western Sierras Pampeanas
ESP Eastern Sierras Pampeanas

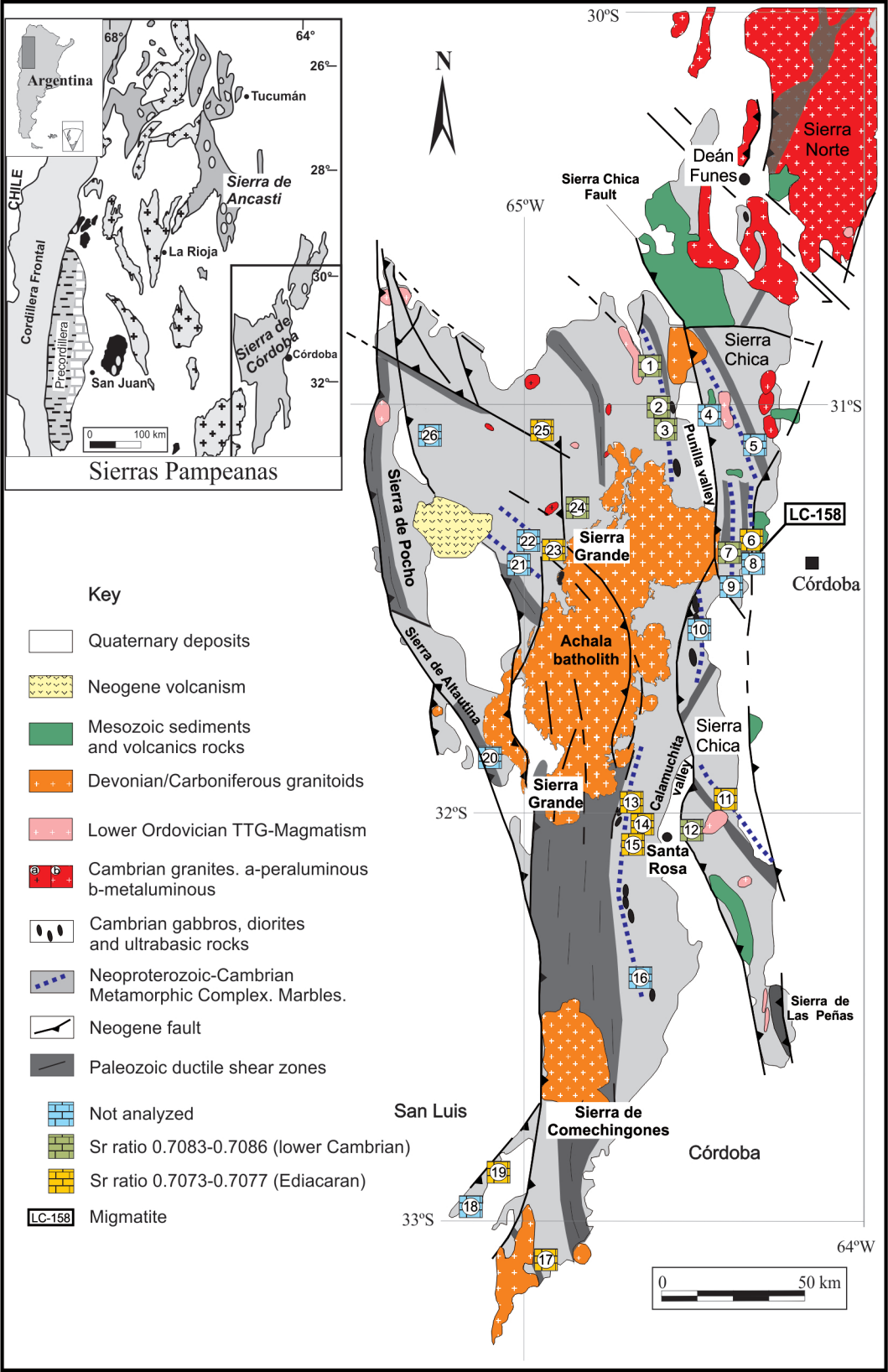
Argentina
CHILE
Cordillera Frontal
Precordillera
Sierra de Ancasti
Tucumán
La Rioja
San Juan
Sierra de Córdoba
Córdoba
68°
64°
26°
28°
30°
32°
0 100 km
Sierras Pampeanas
N
30ºS
65ºW
31ºS
32ºS
33ºS
64ºW
Sierra Norte
Deán Funes
Sierra Chica Fault
Sierra Chica
Punilla valley
LC-158
Córdoba
Sierra de Pocho
Sierra de Altautina
Sierra Grande
Achala batholith
Calamuchita valley
Santa Rosa
Sierra de Las Peñas
San Luis
Sierra de Comechingones
0 50 km
Key
Quaternary deposits
Neogene volcanism
Mesozoic sediments and volcanics rocks
Devonian/Carboniferous granitoids
Lower Ordovician TTG-Magmatism
a b
Cambrian granites. a-peraluminous b-metaluminous
Cambrian gabbros, diorites and ultrabasic rocks
Neoproterozoic-Cambrian Metamorphic Complex. Marbles.
Neogene fault
Paleozoic ductile shear zones
Not analyzed
Sr ratio 0.7083-0.7086 (lower Cambrian)
Sr ratio 0.7073-0.7077 (Ediacaran)
LC-158
Migmatite

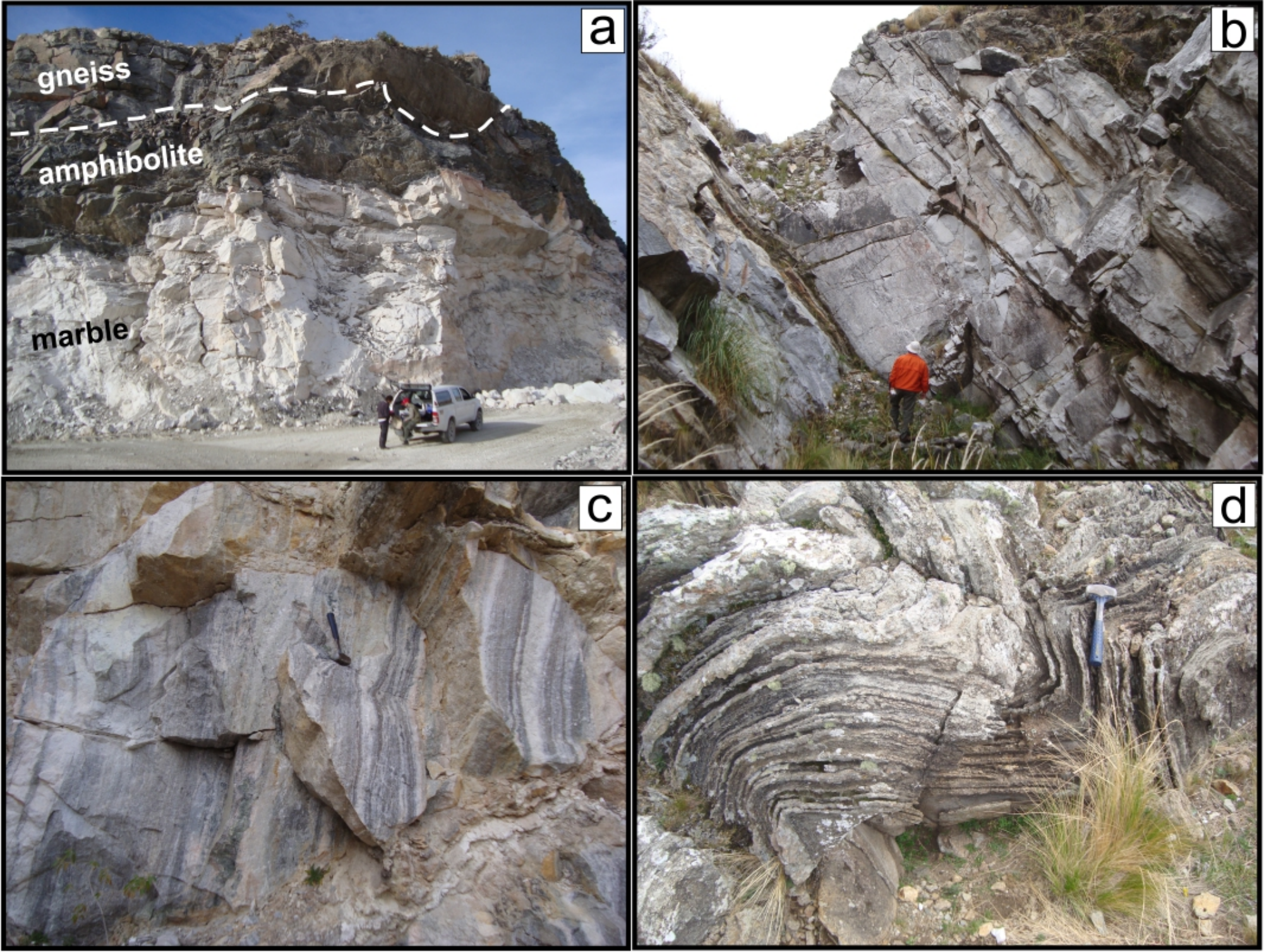
a
gneiss
amphibolite
marble
b
c
d

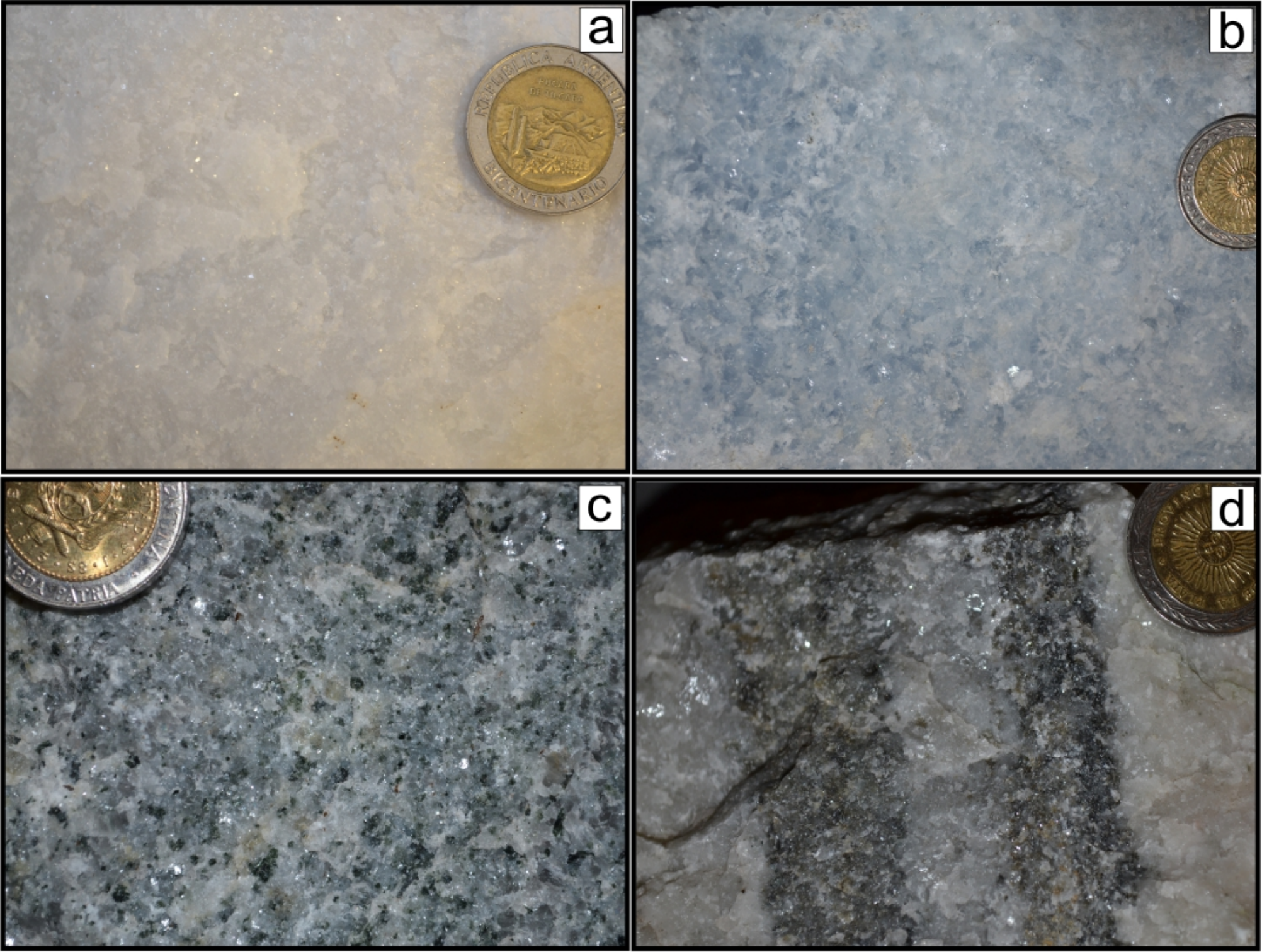
a
b
c
d

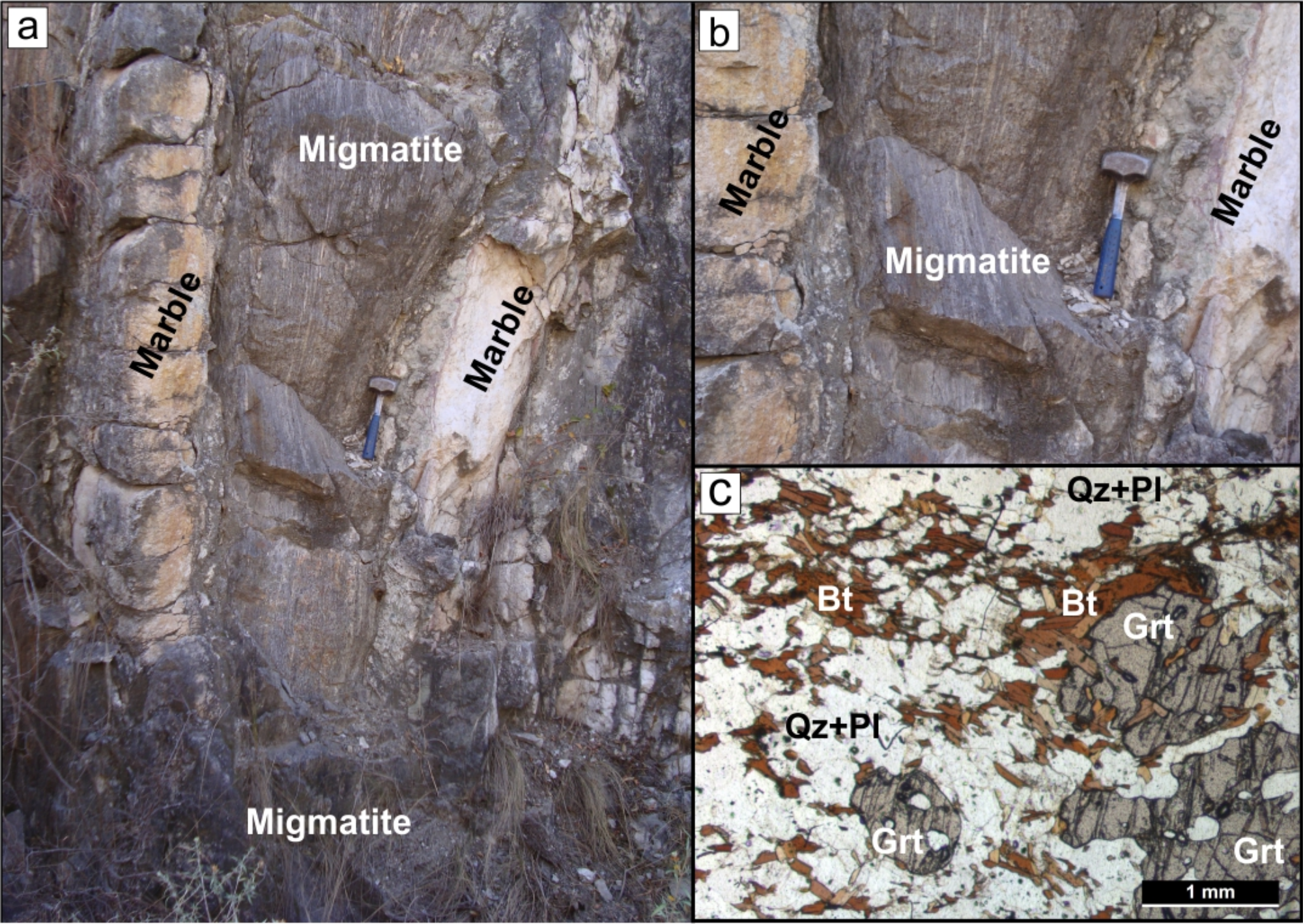
a
Migmatite
Marble
Marble
Migmatite
b
Marble
Marble
Migmatite
c
Qz+Pl
Bt
Bt
Grt
Qz+Pl
Grt
Grt
1 mm

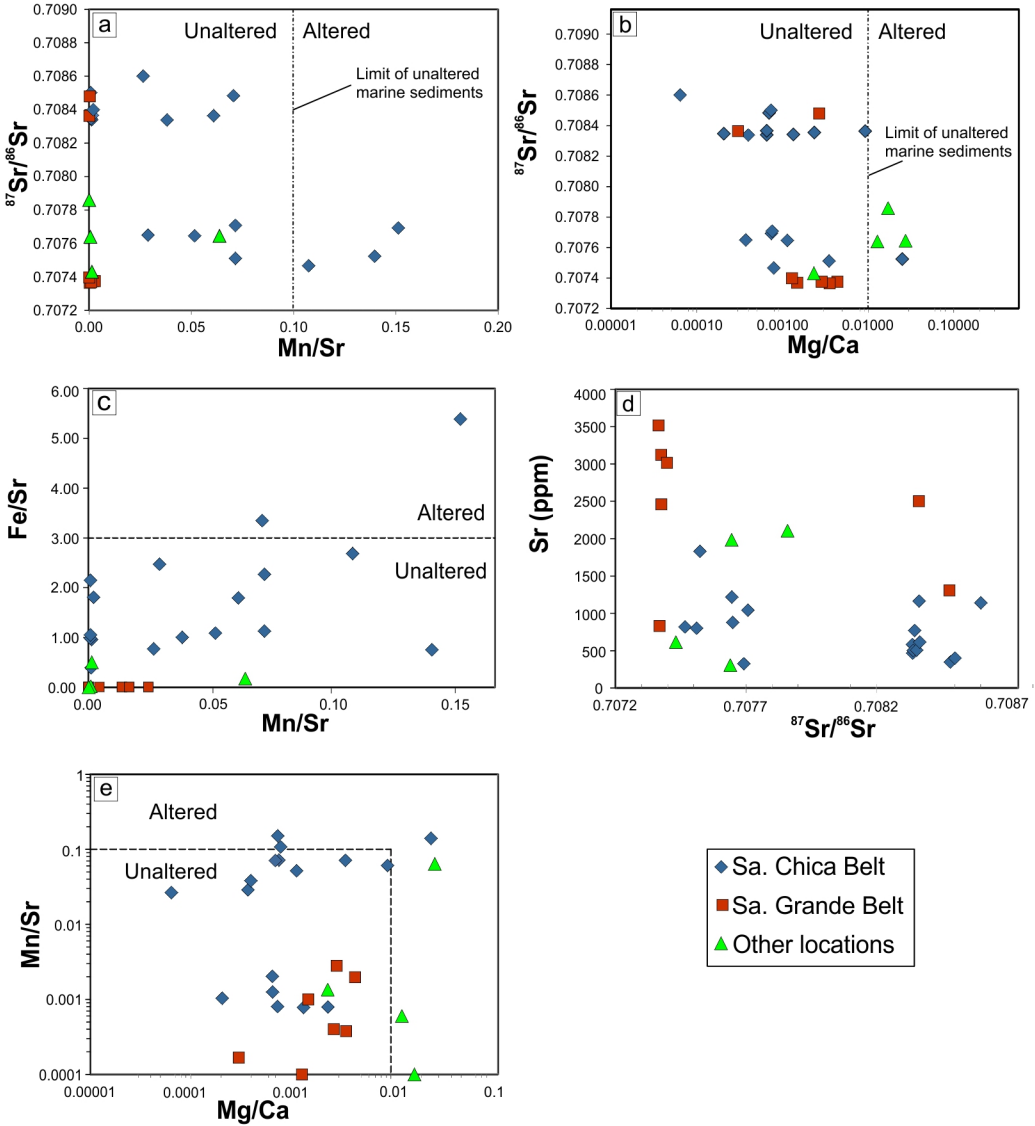
a
Unaltered
Altered
Limit of unaltered marine sediments
$^{87}Sr/^{86}Sr$
Mn/Sr
b
Unaltered
Altered
Limit of unaltered marine sediments
$^{87}Sr/^{86}Sr$
Mg/Ca
c
Altered
Unaltered
Fe/Sr
Mn/Sr
d
Sr (ppm)
$^{87}Sr/^{86}Sr$
e
Altered
Unaltered
Mn/Sr
Mg/Ca
Sa. Chica Belt
Sa. Grande Belt
Other locations


a
LC-51
710
LC-19
946
LC-8
1191
LC-9
1198
LC-15
1564
LC-21
1665
LC-39
864
LC-2
918
LC-22
1324
LC-12
1885
LC-38
1168
LC-11
1328
LC-30
1458
LC-1
1998
LC-20
1158
LC-18
1082
LC-55
1213
LC-53
1208
LC-17
2014
100 µm
b
LC-26
534
LC-44
529
LC-32
534
LC-35
533
LC-43
525
LC-41
528
LC-42
529
LC-34
533
LC-54
526
LC-23
514
LC-46
525
LC-36
526
LC-48
308
LC-49
524
100 µm

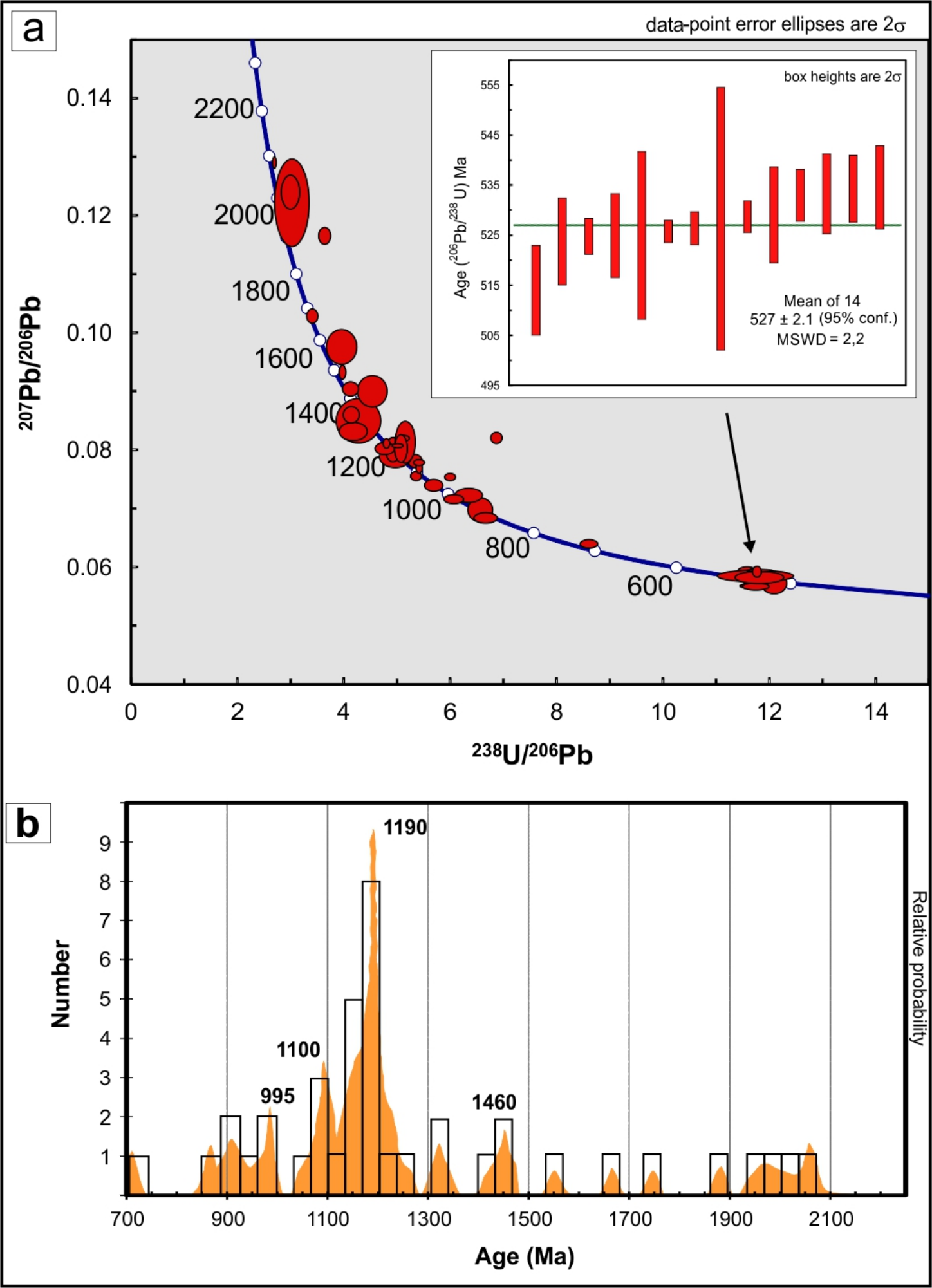
a
data-point error ellipses are 2σ
box heights are 2σ
Age (^{206}Pb/^{238}U) Ma
555
545
535
525
515
505
495
Mean of 14
527 ± 2.1 (95% conf.)
MSWD = 2,2
^{207}Pb/^{206}Pb
0.14
0.12
0.10
0.08
0.06
0.04
2200
2000
1800
1600
1400
1200
1000
800
600
0
2
4
6
8
10
12
14
^{238}U/^{206}Pb
b
Number
9
8
7
6
5
4
3
2
1
1190
1100
995
1460
700
900
1100
1300
1500
1700
1900
2100
Age (Ma)
Relative probability

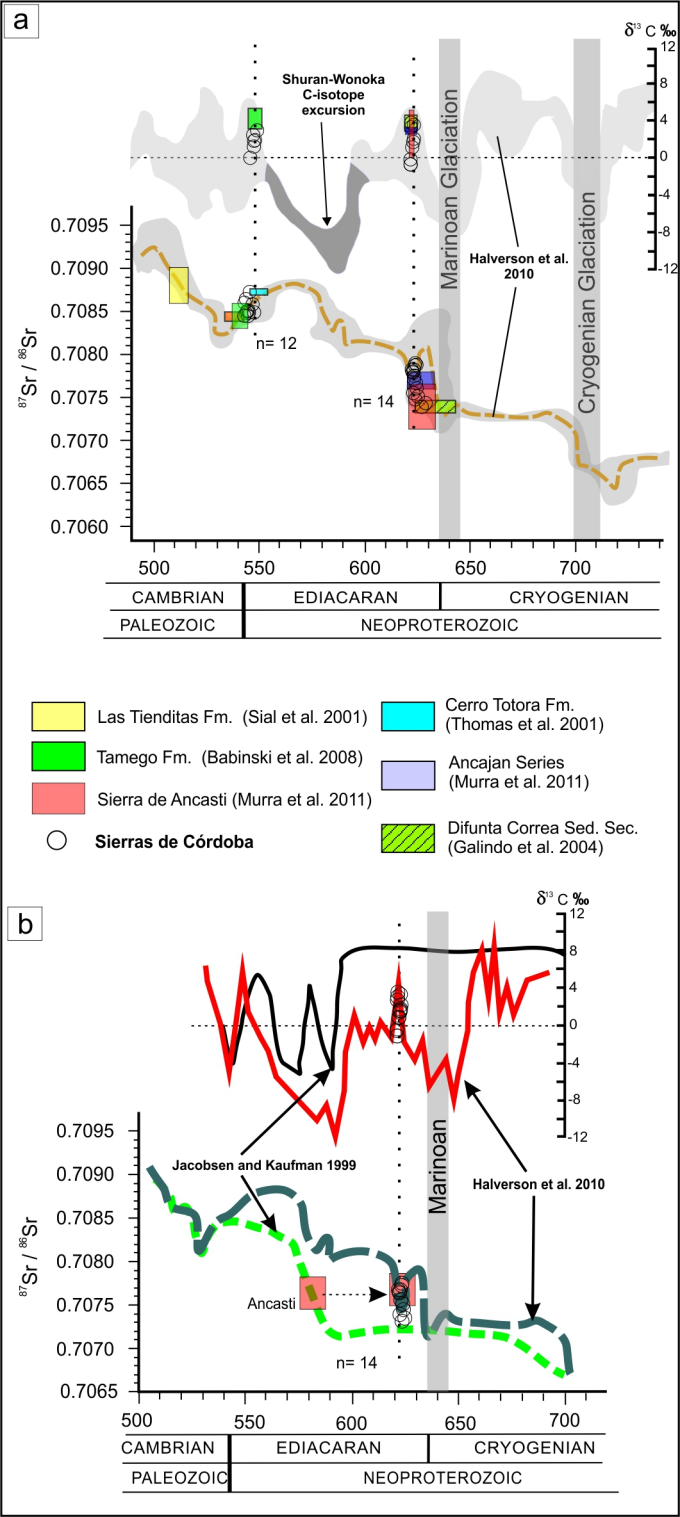
a
δ13 C ‰
12
8
4
0
-4
-8
-12
Shuran-Wonoka
C-isotope
excursion
Marinoan Glaciation
Cryogenian Glaciation
Halverson et al.
2010
0.7095
0.7090
0.7085
0.7080
0.7075
0.7070
0.7065
0.7060
87Sr / 86Sr
n= 12
n= 14
500
550
600
650
700
CAMBRIAN
EDIACARAN
CRYOGENIAN
PALEOZOIC
NEOPROTEROZOIC
Las Tienditas Fm. (Sial et al. 2001)
Tamego Fm. (Babinski et al. 2008)
Sierra de Ancasti (Murra et al. 2011)
Sierras de Córdoba
Cerro Totora Fm.
(Thomas et al. 2001)
Ancajan Series
(Murra et al. 2011)
Difunta Correa Sed. Sec.
(Galindo et al. 2004)
b
δ13 C ‰
12
8
4
0
-4
-8
-12
Jacobsen and Kaufman 1999
Marinoan
Halverson et al. 2010
0.7095
0.7090
0.7085
0.7080
0.7075
0.7070
0.7065
87Sr / 86Sr
Ancasti
n= 14
500
550
600
650
700
CAMBRIAN
EDIACARAN
CRYOGENIAN
PALEOZOIC
NEOPROTEROZOIC

Table 1. Location, field description and petrography of marbles and migmatite LC-158. * Not analyzed for geochemistry.

Sample	latitude	longitude		Location	Rock description	% Calcite (staining)	Mineralogy (mineral abbreviation after Whitney and Evans 2010)
CUA50 *	31°07'37.2"	64°25'25.9"	Sierra Chica Belt	El Cuadrado	white, massive, middle-grained	54.67	Cal-Dol-Qz-Srp
ES01 *	31°5'31.9"	64°19'21.3"		El Sauce	green, banded, middle-grained	9.18	Dol-Cal-Srp-Phl-Di-Ep-Chl-Tr-Qz-Opq
Q01 *	30°51'58.1"	64°41'06.5"		Quilpo	bluish, massive, coarse-grained	69.87	Cal-Dol-Di-Wo-Qz-Phl-Opq
Q02	30°51'58.1"	64°41'06.5"			pinkish, massive, coarse-grained	98.1	Cal-Qz-Phl-Ttn-Tr-Tlc
Q04b	30°51'58.1"	64°41'06.5"			white, massive, fine-grained	97.64	Cal-Qz-Tlc-Di
Q08	30°51'55.9"	64°41'32.7"			white, massive, coarse-grained	98.5	Cal-Qz-Phl-Di-Tlc-Opq
Q09	30°51'55.9"	64°41'32.7"			pinkish, massive, coarse-grained	93.58	Cal-Qz-Ttn-Phl-Tcl
Q14	30°52'1.5"	64°40'58.6"			white, massive, coarse-grained	98.62	Cal-Qz-Ttn-Phl-Tlc
Q21	31°02'0.3"	64°33'39.6"		Centenario	pinkish, massive, coarse-grained	92.1	Cal-Dol-Qz-Di-Phl-Opq-Ol-Srp
Q22 *	31°02'0.3"	64°33'39.6"			white, massive, coarse-grained	67.75	Cal-Dol-Qz-Ttn-Phl
Q25b	31°5'53.1"	64°31'56.3"		La Falda	white, massive, coarse-grained	97.57	Cal-Qz-Phl-Ap-Opq-Ttn
Q27	31°5'53.1"	64°31'56.3"			pinkish, massive, coarse-grained	97.84	Cal-Dol-Qz-Ttn-Di-Phl-Tlc
AG03 *	31°38'20.9"	64°28'52.8"		Alta Gracia	white, banded, middle-grained	19.2	Cal-Dol-Ol-Di-Phl-Srp
AG04 *	31°40'20.8"	64°26'37.8"			gray, banded, middle to fine-grained	68.7	Cal-Dol-Ol-Phl-Di-Srp-Opq
CAN35	31°21'10.1"	64°20'58"		Cantesur	white to pinkish, fine-grained, mylonitized	96.68	Cal-Di-Ttn-Tr-Pl-Qz
D32	31°18'31.7"	64°20'05.2"		Dumesnil	white to pinkish, massive, middle-grained	99.5	Cal-Dol-Qz-Phl-Di
D33 *	31°18'31.7"	64°20'05.2"			white, massive, fine-grained	45.3	Cal-Dol-Srp-Phl
D37	31°18'31.7"	64°20'05.2"			pinkish, banded, coarse-grained	98.23	Cal-Grt-Qz-Phl-Opq-Di
D38 *	31°18'31.7"	64°20'05.2"			pinkish, massive, middle-grained	48.84	Cal-Dol-Srp-Ol-Di
D40	31°18'31.7"	64°20'05.2"			white, massive, coarse-grained	97.83	Cal-Qz-Opq-Tr-Phl-Mc-Di
D41 *	31°18'31.7"	64°20'05.2"			white, massive, middle-grained	77.95	Cal-Dol-Srp-Ol-Phl
LC-158 *	31º21'37.6"	64º20'59.7"		La Calera	granoblastic/ lepidoblastic lenses - fine to middle-grained	no data	Qz-Grt-Pl-Bt- ±Sil-[Zrn-Ep-Opq-Ap]
LJ143 *	31°35'29.6"	64°34'59.4"		Las Jarillas	white, massive, coarse-grained	12.17	Dol-Tr-Phl-Chl-Cal
CA69 *	32°24'37.4"	64°31'55.6"		Cañada de Alvarez	white, massive, coarse-grained	15.68	Dol-Phl-Ser-Tr-±Cal
CA71a *	32°24'10.1"	64°31'44.8"			bluish, massive, coarse-grained	9.21	Dol-Srp-Di-Phl-Ol-±Cal
SA1 *	32°00'10.5"	64°24'29.1"		San Agustín	white, banded, coarse-grained	0.5	Dol-Phl-Srp-Tlc-Chl
SA56	31°56'12.9"	64°25'9.9"			white, massive, fine-grained	98.54	Cal-Qz-Tr-Opq
SM81 *	32°03'30"	64°41'45.4"		Sta. Mónica	white, massive, coarse-grained	84.02	Cal-Dol-Iddingsite
SM82	32°03'30"	64°41'45.4"			pinkish, banded, coarse-grained	95.06	Cal-Qz-Ttn-Phl
SMi87	32°02'48.4"	64°43'57"		San Miguel	pinkish, banded, fine-grained	96	Cal-Qz-Pl-Ttn-Di-Tr-Phl
SOL91 *	31°59'25.8"	64°43'32.6"		Sol de Mayo	white, banded, fine-grained	83.78	Cal-Dol-Pl-Srp-Qz
SOL92	31°59'25.8"	64°43'32.6"			white, banded, coarse-grained	92.02	Cal-Phl-Qz-Tr-Di-Dol
SR77 *	32°04'50"	64°27'59.8"		Sta. Rosa	white, massive, fine-grained	69.33	Cal-Phl-Qz-Anf-Iddingsita
SR79	32°04'50"	64°27'59.8"			white, massive, coarse-grained	95	Cal-Qz-Di-Ttn-Gr
AL135 *	31°45'53.7"	65°09'21.4"	Sierra Grande Belt	Altautina	white, massive, coarse-grained	8.85	Dol-Phl-Di-Tr±Cal
BN	31°7'57.2"	64°46'48.3"		Characato	bluish, massive, coarse-grained	79.35	Cal-Qtz-Tr-Di-Opq-Ttn±Dol
CU126 *	31°19'48.2"	65°01'54.9"		Cuchiyaco	white, banded, middle-grained	18.79	Dol-Cal-Tlc-Phl-Di-Srp-Ol-Spl-Opq
IG101	31°15'3.20"	64°49'11.1"		Igam	white, massive, coarse-grained	74.6	Cal-Qz-Di-±Dol
IG102	31°15'3.20"	64°49'11.1"			gray, massive, coarse-grained	73.46	Cal-Tr-Qz-Opq-±Dol
IG104	31°15'3.20"	64°49'11.1"			gray, banded, middle to fine-grained	81.98	Cal-Qtz-Tr-Di-Opq-Ttn±Dol
IGU178	31º03'49"	64º47'34.1"		Iguazú	gray, massive, coarse-grained	93.16	Cal-Qz-Opq
IGU179	31º03'49"	64º47'34.1"			gray, banded, middle-grained	76.61	Cal-Qz-Opq-Tr±Dol
IGU180*	31º01'03.7"	64º50'32.6"			gray, banded, middle to fine-grained	97.35	Cal-Qz-Opq-Tr-Phl
SG172	31º05'35.4"	64º48'27.2"		San Gregorio	white, massive, coarse-grained	97.48	Cal-Phl-Qz
TC121 *	31°22'44.2"	65°03'11.5"		Tala Cañada	white, massive, fine-grained	26.9	Dol-Di-Opq-Qz-Cal
LC193*	32º56'34.8"	65º08'18.7"	Other locations	San Luis	gray, massive, fine-grained	74.12	Cal-Tr-Qz-Gr±Dol
LC194	32º56'34.8"	65º08'18.7"			gray, banded, middle to fine-grained	93.04	Cal-Tr-Qz-Gr
LC195	32º56'34.8"	65º08'18.7"			gray, massive, coarse-grained	85.28	Cal-Tr-Qz-Gr±Dol
AC60	33°08'43.1"	64°57'15.9"		Achiras	white, massive, fine-grained	75.5	Cal-Dol-Qz-Tr-Phl-Di-Phl
AC61a	33°08'43.1"	64°57'15.9"			gray, banded, middle to fine-grained	97.36	Cal-Dol-Tr-Phl-Qz

Table 2. Elemental and isotopic composition of Sr, C and O marbles. [IR %]: Insoluble residue.
n.d. = no detected

Sample	Location		Rb (ppm)	Sr (ppm)	$^{87}Sr/^{86}Sr$	$\delta^{13} C_{PDB}$ ‰	$\delta^{18} O_{PDB}$ ‰	Ca % weight	Mg % weight	Fe (ppm)	Mn (ppm)	Mg/Ca	Mn/Sr	IR %
Q02	Sierra Chica Belt	Quilpo	<0.2	499	0.70834			42.33	0.057	489	0.39	0.0013	0.0008	2
Q04b				767	0.70835	1.89	-6.54	44.15	0.009	297	0.79	0.0002	0.001	0.14
Q08			<0.2	505	0.70835			42.42	0.1	528	0.4	0.0024	0.0008	0.26
Q09				612	0.70837	1.63	-10.84	45.05	0.03	1105	1.24	0.0007	0.002	1.88
Q14				581	0.70834			51.41	0.021	579	22.12	0.0004	0.0381	2.65
Q21		Centenario	<0.2	344	0.70848			46.12	0.032	1149	24.29	0.0007	0.0706	2.53
Q25b		La Falda		463	0.70834	2.03	-6.14	43.28	0.029	441	0.58	0.0007	0.0012	0.96
Q27				1162	0.70836	1.74	-8.05	31.39	0.292	2080	70.86	0.0093	0.0609	4.47
CAN35		Cantesur		398	0.70850	0.81	-9.14	41.26	0.031	852	0.32	0.0007	0.0008	2.14
D32		Dumesnil		1214	0.70765	-1.05	-8.06	42.86	0.049	1319	62.7	0.0011	0.0516	0.18
D37				1038	0.70771	-0.91	-7.8	45.53	0.035	2351	74.29	0.0008	0.0715	0.57
D40				876	0.70765	-0.59	-6.03	43.82	0.016	2161	25.28	0.0004	0.0288	0.4
SA56		San Agustín		324	0.70769	-0.16	-8.88	39.88	0.03	1742	48.93	0.0007	0.1512	1.2
SM82		Sta. Mónica		816	0.70747	1.96	-9.32	44.58	0.036	2187	87.67	0.0008	0.1074	2.49
SMi87		San Miguel		1828	0.70752	3.25	-12.05	30.45	0.768	1366	255.29	0.0252	0.1396	3.87
SOL92		Sol de Mayo		797	0.70751	3.54	-10.4	37.74	0.133	896	57.02	0.0035	0.0715	1.63
SR79		Sta. Rosa		1137	0.70860	1.07	-8.74	38.04	0.002	873	30.1	0.0001	0.0265	1.54
BN	Sierra Grande Belt	Characato		2497	0.70836	0.73	-5.25	34.36	0.01	11	0.42	0.0003	0.0002	1.5
IG101		Igam		2456	0.70737			31.92	0.141	59	4.84	0.0044	0.0019	2.7
IG102				3513	0.70736	2.98	-5.14	32.51	0.117	47	1.32	0.0036	0.0004	3.09
IG104				3120	0.70737	3.09	-4.86	33.50	0.097	51	8.71	0.0029	0.0028	2.1
SG172		San Gregorio	<0.2	1304	0.70848			40.77	0.11	n.d	0.59	0.0027	0.0004	1.94
IGU178		Iguazú		828	0.70737	3.2	-9.14	32.84	0.507	n.d	0.86	0.0015	0.0010	1.48
IGU179				3012	0.70740			33.35	0.456	n.d	0.35	0.0013	0.0001	7.58
AC60	Other locations	Achiras		1981	0.70764	2.78	-7.91	27.95	0.771	343	126.28	0.0276	0.0637	4.03
AC61a				613	0.70743			35.28	0.083	305	0.83	0.0023	0.0013	1.25
LC194		San Luis		305	0.70764			33.85	0.438	n.d	0.2	0.0129	0.0006	5.48
LC195				2106	0.70786			35.52	0.611	n.d	0.22	0.0172	0.0001	6.03

Table 3. Summary of SHRIMP U-Pb zircon results for sample LC-158

						Total ratios				Radiogenic Ratios							Ages					Preferred age (Ma)	
Grain spot	U ppm	Th ppm	Th/U	206Pb ppm	f_{206} %	207Pb/ 206Pb	±	206Pb/ 238U	±	206Pb/ 238U	±	207Pb/ 206Pb	±	207Pb/ 235U	±	ρ	206Pb/ 238U	±	207Pb/ 206Pb	±	% Disc		±
1	155.7	114.4	0.75	42.0	-0.15	0.12180	0.00214	0.31175	0.00527	0.12288	0.00246	0.31214	0.00529	5.28827	0.13994	0.461	1751.2	26.0	1998.5	35.0	12.4	1751.2	26.0
2	173.7	46.7	0.28	23.0	0.13	0.06962	0.00164	0.15303	0.00438	0.15302	0.00487	0.04470	0.00139				917.9	27.3				917.9	27.3
3	67.8	55.7	0.84	21.9	0.23	0.12893	0.00082	0.37410	0.00356	0.12723	0.00082	0.37338	0.00355	6.55029	0.07883	0.569	2045.3	16.7	2060.1	11.4	0.7	2060.1	11.4
5	111.7	57.1	0.52	32.1	-0.19	0.11906	0.00164	0.33166	0.00911	0.12045	0.00166	0.33219	0.00912	5.51674	0.17066	0.639	1849.0	44.3	1962.9	24.4	5.8	1962.9	24.4
6	76.1	31.0	0.42	13.0	0.00	0.07976	0.00014	0.19699	0.00477	0.07976	0.00014	0.19699	0.00477	2.16628	0.05315	0.710	1159.1	25.7	1191.1	3.4	2.7	1191.1	3.4
7	538.6	433.5	0.83	155.2	-0.01	0.12205	0.00611	0.33300	0.02941	0.12212	0.00611	0.33303	0.02941	5.60771	0.56964	0.626	1853.0	143.8	1987.5	86.4	6.8	1987.5	86.4
8	191.1	95.1	0.51	33.5	0.02	0.07991	0.00089	0.20234	0.00218	0.07977	0.00090	0.20231	0.00218	2.22507	0.03574	0.484	1187.7	11.7	1191.3	22.2	0.3	1187.7	11.7
9	266.3	154.8	0.60	46.9	0.13	0.08109	0.00072	0.20367	0.00343	0.08004	0.00072	0.20342	0.00342	2.24483	0.04362	0.623	1193.6	18.3	1197.9	17.8	0.4	1197.9	17.8
10	86.5	38.2	0.45	11.3	-0.09	0.06829	0.00072	0.15062	0.00407	0.15079	0.00436	0.04345	0.00210				905.4	24.5				905.4	24.5
11	177.8	89.7	0.52	36.2	-0.09	0.08481	0.00310	0.23496	0.01880	0.08553	0.00310	0.23515	0.01882	2.77331	0.24384	0.655	1361.5	99.0	1327.7	68.6	-2.5	1327.7	68.6
12	136.8	187.4	1.41	32.8	0.13	0.11635	0.00121	0.27684	0.00719	0.11535	0.00125	0.27651	0.00718	4.39786	0.12480	0.659	1573.8	36.4	1885.3	19.4	16.5	1885.3	19.4
13	73.3	26.9	0.38	12.7	0.16	0.07973	0.00067	0.19995	0.00599	0.07850	0.00088	0.19966	0.00598	2.16100	0.06951	0.671	1173.5	32.2	1159.5	22.0	-1.2	1159.5	22.0
14	93.0	39.7	0.44	16.1	0.00	0.07801	0.00075	0.20047	0.00572	0.07801	0.00075	0.20047	0.00572	2.15630	0.06540	0.678	1177.8	30.8	1147.1	19.0	-2.7	1147.1	19.0
15	125.6	26.5	0.22	27.6	0.07	0.09742	0.00242	0.25371	0.01498	0.09686	0.00246	0.25355	0.01497	3.38605	0.21802	0.660	1456.7	77.4	1564.5	46.8	6.9	1564.5	46.8
16	168.6	78.3	0.48	35.2	0.00	0.08302	0.00123	0.24086	0.01231	0.08300	0.00131	0.24086	0.01231	2.75634	0.14775	0.686	1391.1	64.2	1269.1	30.6	-9.6	1269.1	30.6
17	147.4	128.5	0.89	42.9	-0.01	0.12386	0.00240	0.33618	0.01625	0.12397	0.00241	0.33622	0.01625	5.74715	0.30003	0.667	1868.5	78.9	2014.1	34.0	7.2	2014.1	34.0
18	238.3	181.1	0.78	38.7	-0.01	0.07543	0.00062	0.18759	0.00296	0.07551	0.00062	0.18760	0.00296	1.95326	0.03542	0.627	1108.4	16.1	1082.1	16.4	-2.4	1082.1	16.4
19	97.0	182.9	1.93	13.3	0.47	0.07212	0.00097	0.15831	0.00517	0.15799	0.00557	0.04647	0.00174				945.6	31.1				945.6	31.1
20	164.2	69.5	0.43	26.7	-0.07	0.07790	0.00090	0.18813	0.00401	0.07845	0.00092	0.18825	0.00401	2.03613	0.04998	0.625	1111.9	21.8	1158.3	22.8	4.0	1111.9	21.8
21	195.3	146.9	0.77	49.9	0.07	0.10273	0.00098	0.29533	0.00716	0.10221	0.00101	0.29515	0.00716	4.15943	0.10994	0.661	1667.2	35.7	1664.7	18.0	-0.2	1664.7	18.0
22	195.3	100.3	0.53	41.0	0.06	0.08586	0.00114	0.24287	0.00703	0.08536	0.00114	0.24273	0.00703	2.85675	0.09171	0.649	1400.9	36.6	1323.7	25.8	-5.8	1323.7	25.8
23	253.1	13.9	0.06	18.2	0.27	0.05708	0.00147	0.08293	0.00132	0.08298	0.00151	0.02442	0.00047				513.9	9.0				513.9	9.0
24	107.5	32.3	0.31	18.8	0.52	0.07871	0.00152	0.20235	0.01002	0.07465	0.00207	0.20139	0.00998	2.07277	0.11785	0.627	1182.8	53.8	1059.1	54.6	-11.7	1182.8	53.8
25	47.4	53.6	1.16	9.1	0.15	0.08988	0.00220	0.22174	0.01102	0.08871	0.00291	0.22143	0.01101	2.70839	0.16159	0.600	1289.4	58.3	1397.9	61.6	7.8	1397.9	61.6
26	291.9	9.7	0.03	21.9	0.14	0.05923	0.00056	0.08653	0.00105	0.08640	0.00114	0.02431	0.00056				534.2	6.7				534.2	6.7
27	74.8	35.8	0.49	10.7	0.00	0.07147	0.00066	0.16536	0.00418	0.16547	0.00450	0.05102	0.00146				987.1	24.9				987.1	24.9
28	119.1	126.3	1.09	19.1	0.30	0.07687	0.00082	0.18543	0.00162	0.07448	0.00088	0.18490	0.00161	1.89888	0.02865	0.416	1095.3	10.3				1095.3	10.3
29	157.1	53.5	0.35	24.0	0.04	0.07382	0.00086	0.17622	0.00444	0.07347	0.00107	0.17615	0.00444	1.78436	0.05237	0.618	1046.7	26.7				1046.7	26.7
30	98.9	35.6	0.37	20.9	-0.16	0.09028	0.00100	0.24371	0.00759	0.09154	0.00168	0.24407	0.00761	3.08068	0.11194	0.618	1407.8	39.5	1457.9	34.4	3.4	1457.9	34.4
31	325.6	84.4	0.27	57.4	0.03	0.07966	0.00044	0.20352	0.00289	0.07943	0.00046	0.20347	0.00289	2.22836	0.03516	0.648	1193.9	15.5	1182.9	11.6	-0.9	1182.9	11.6
32	343.9	16.6	0.05	25.7	0.39	0.05838	0.00064	0.08648	0.00130	0.08645	0.00140	0.03193	0.00080				534.5	8.3				534.5	8.3
33	115.1	57.9	0.52	18.5	0.09	0.07773	0.00048	0.18546	0.00306	0.07702	0.00057	0.18530	0.00306	1.96787	0.03634	0.644	1094.3	18.2				1094.3	18.2
34	331.0	11.6	0.04	24.7	0.09	0.05725	0.00083	0.08610	0.00077	0.08618	0.00087	0.02768	0.00270				532.9	5.2				532.9	5.2
35	204.1	9.8	0.05	15.2	0.00	0.05670	0.00031	0.08608	0.00127	0.08623	0.00134	0.02984	0.00331				533.2	8.0				533.2	8.0
36	302.4	9.7	0.03	22.2	0.21	0.05753	0.00020	0.08494	0.00033	0.08496	0.00036	0.02720	0.00214				525.7	2.2				525.7	2.2
37	264.8	12.8	0.05	19.5	-0.01	0.05837	0.00079	0.08489	0.00131	0.08481	0.00141	0.02492	0.00054				524.8	8.4				524.8	8.4
38	112.5	46.6	0.42	19.9	0.14	0.07995	0.00173	0.20434	0.00458	0.07885	0.00177	0.20407	0.00458	2.21876	0.07094	0.505	1197.2	24.6	1168.5	43.8	-2.5	1197.2	24.6
39	557.4	27.3	0.05	70.5	0.05	0.08188	0.00080	0.14618	0.00181	0.08152	0.00082	0.14611	0.00181	1.64240	0.02686	0.546	864.4	12.2				864.4	12.2
40	356.8	98.4	0.28	60.2	0.25	0.08118	0.00288	0.19504	0.00570	0.07920	0.00297	0.19458	0.00569	2.12494	0.10137	0.441	1146.2	30.8	1177.1	72.6	2.6	1146.2	30.8
41	517.3	18.7	0.04	38.3	0.00	0.05833	0.00079	0.08543	0.00426	0.08539	0.00442	0.02905	0.00292				528.2	26.3				528.2	26.3
42	272.7	12.2	0.05	20.2	0.07	0.05935	0.00018	0.08562	0.00052	0.08545	0.00053	0.02804	0.00023				528.6	3.2				528.6	3.2
43	349.1	12.1	0.04	25.6	0.12	0.05814	0.00046	0.08483	0.00053	0.08480	0.00060	0.02545	0.00106				524.7	3.6				524.7	3.6
44	278.0	11.0	0.04	20.5	0.00	0.05657	0.00048	0.08537	0.00154	0.08552	0.00162	0.02569	0.00141				529.0	9.6				529.0	9.6
45	153.4	58.3	0.39	33.6	0.07	0.09310	0.00099	0.25299	0.00335	0.09255	0.00100	0.25283	0.00335	3.22614	0.05643	0.545	1453.0	17.2	1478.7	20.4	1.7	1453.0	17.2
46	389.4	11.1	0.03	28.6	0.08	0.05812	0.00083	0.08486	0.00269	0.08483	0.00283	0.02556	0.00136				524.9	16.8				524.9	16.8
47	153.2	65.9	0.44	27.9	0.07	0.08008	0.00089	0.21043	0.00637	0.07955	0.00093	0.21030	0.00637	2.30669	0.07532	0.668	1230.4	34.0	1185.9	23.0	-3.8	1185.9	23.0
48	261.0	170.4	0.67	11.1	0.05	0.05277	0.00107	0.04895	0.00077	0.04894	0.00086	0.01523	0.00028				308.0	5.3				308.0	5.3
49	458.2	10.5	0.02	33.6	0.19	0.05924	0.00020	0.08480	0.00143	0.08463	0.00146	0.03023	0.00094				523.7	8.7				523.7	8.7
50	275.3	38.4	0.14	39.9	-0.05	0.07525	0.00050	0.16751	0.00229	0.16686	0.00249	0.04796	0.00075				994.8	13.8				994.8	13.8
51	196.8	108.1	0.56	19.8	-0.15	0.06381	0.00059	0.11653	0.00181	0.11641	0.00195	0.03399	0.00058				709.9	11.3				709.9	11.3
52	129.9	34.7	0.27	22.0	0.12	0.08186	0.00039	0.19562	0.00337	0.08095	0.00150	0.19541	0.00338	2.18120	0.05580	0.487	1150.6	18.2	1220.3	36.0	5.7	1150.6	18.2
53	217.1	62.6	0.30	39.4	0.07	0.08102	0.00068	0.20961	0.00212	0.08047	0.00070	0.20947	0.00212	2.32411	0.03205	0.528	1226.0	11.3	1208.5	17.0	-1.4	1226.0	11.3
54	264.8	11.8	0.05	19.5	0.20	0.05905	0.00074	0.08520	0.00048	0.08507	0.00056	0.03001	0.00072				526.3	3.3				526.3	3.3
55	171.9	70.7	0.42	29.5	-0.08	0.08006	0.00191	0.19825	0.00393	0.08064	0.00193	0.19839	0.00394	2.20588	0.06914	0.456	1166.6	21.2	1212.7	46.6	3.8	1166.6	21.2
56	262.7	66.5	0.26	45.6	0.08	0.08058	0.00024	0.20049	0.00348	0.07995	0.00042	0.20034	0.00348	2.20854	0.04081	0.676	1177.2	18.7	1195.7	10.4	1.5	1195.7	10.4

Notes: 1. Uncertainties given at the two σ level

2. for areas younger than 1100 Ma correction for common Pb made using the measured $^{238}U/^{206}Pb$ and $^{207}Pb/^{206}Pb$ ratios

3. for areas older than 1100 Ma correction for common Pb made using the measured $^{204}Pb/^{206}Pb$